

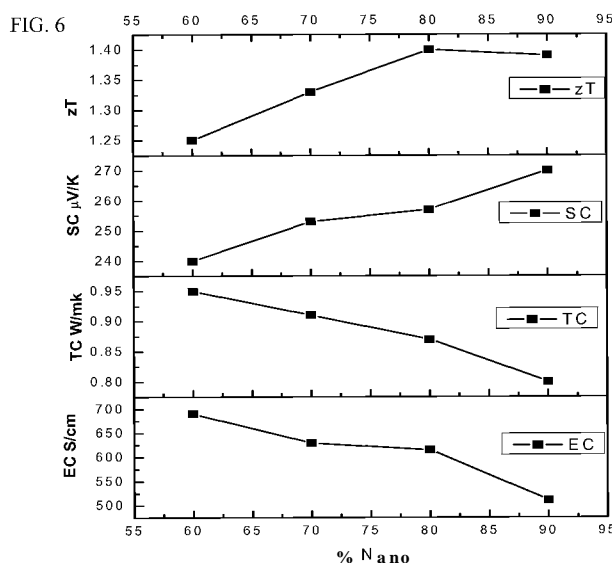


- (51) **International Patent Classification:**  
*H01L 35/18* (2006.01)
- (21) **International Application Number:**  
PCT/US2013/042537
- (22) **International Filing Date:**  
23 May 2013 (23.05.2013)
- (25) **Filing Language:** English
- (26) **Publication Language:** English
- (30) **Priority Data:**  
3024/DEL/2012 27 September 2012 (27.09.2012) IN  
1002/CHE/2013 8 March 2013 (08.03.2013) IN
- (71) **Applicant: LAIRD TECHNOLOGIES, INC.** [US/US];  
3481 Rider Trail South, Earth City, MO 63045 (US).
- (72) **Inventors: KHANDERI, Jayaprakash;** 3481 Rider Trail  
South, Earth City, MO 63045 (US). **PURKAYASTHA, Arup;**  
3481 Rider Trail South, Earth City, MO 63045 (US). **PURUSHOTTAM, Joshi;** 3481 Rider Trail South,  
Earth City, MO 63045 (US).
- (74) **Agent: FUSSNER, Anthony, G.;** Harness, Dickey &  
Pierce, PLC, 7700 Bonhomme, Suite 400, St. Louis, MO  
63105 (US).

- (81) **Designated States** (unless otherwise indicated, for every kind of national protection available): AE, AG, AL, AM, AO, AT, AU, AZ, BA, BB, BG, BH, BN, BR, BW, BY, BZ, CA, CH, CL, CN, CO, CR, CU, CZ, DE, DK, DM, DO, DZ, EC, EE, EG, ES, FI, GB, GD, GE, GH, GM, GT, HN, HR, HU, ID, IL, IN, IS, JP, KE, KG, KM, KN, KP, KR, KZ, LA, LC, LK, LR, LS, LT, LU, LY, MA, MD, ME, MG, MK, MN, MW, MX, MY, MZ, NA, NG, NI, NO, NZ, OM, PA, PE, PG, PH, PL, PT, QA, RO, RS, RU, RW, SC, SD, SE, SG, SK, SL, SM, ST, SV, SY, TH, TJ, TM, TN, TR, TT, TZ, UA, UG, US, UZ, VC, VN, ZA, ZM, ZW.
- (84) **Designated States** (unless otherwise indicated, for every kind of regional protection available): ARIPO (BW, GH, GM, KE, LR, LS, MW, MZ, NA, RW, SD, SL, SZ, TZ, UG, ZM, ZW), Eurasian (AM, AZ, BY, KG, KZ, RU, TJ, TM), European (AL, AT, BE, BG, CH, CY, CZ, DE, DK, EE, ES, FI, FR, GB, GR, HR, HU, IE, IS, IT, LT, LU, LV, MC, MK, MT, NL, NO, PL, PT, RO, RS, SE, SI, SK, SM, TR), OAPI (BF, BJ, CF, CG, CI, CM, GA, GN, GQ, GW, ML, MR, NE, SN, TD, TG).

**Published:**  
— with international search report (Art. 21(3))

(54) **Title:** BISMUTH ANTIMONY TELLURIDE NANO-BULK COMPOSITES WITH HIGH FIGURES OF MERIT (ZT)



(57) **Abstract:** According to various aspects, exemplary embodiments are disclosed of Bismuth Antimony Telluride (BiSbTe) based nano-bulk composites having high dimensionless figures of merit (ZT) and with nanostructured BiSbTe as the matrix (host) and bulk BiSbTe as the inclusion (guest). In an exemplary embodiment of a thermoelectric nano-bulk composite material, there is a matrix including nanostructured bismuth antimony telluride. The thermoelectric nano-bulk composite material also includes bulk bismuth antimony telluride in the matrix. A weight percentage ratio of the nanostructured bismuth antimony telluride to the bulk bismuth antimony telluride is at least one to one or higher.

WO 2014/051709 A1

## **BISMUTH ANTIMONY TELLURIDE NANO-BULK COMPOSITES WITH HIGH FIGURES OF MERIT (ZT)**

### **CROSS-REFERENCE TO RELATED APPLICATIONS**

[0001] This application claims priority to and the benefit of Indian Patent Application No. 3024/DEL/2012 filed September 27, 2012. This application also claims priority to and the benefit of Indian Patent Application No. 1002/CHE/2013 filed March 8, 2013. The entire disclosures of the above applications are incorporated herein by reference.

### **FIELD**

[0002] The present disclosure relates to Bismuth Antimony Telluride (BiSbTe) based nano-bulk composites having high dimensionless figures of merit (ZT) and with nanostructured BiSbTe as the matrix (host) and bulk BiSbTe as the inclusion (guest). The present disclosure also relates methods of making BiSbTe based nano-bulk composites.

### **BACKGROUND**

[0003] This section provides background information related to the present disclosure which is not necessarily prior art.

[0004] Thermoelectric materials convert thermal energy directly into electrical energy or vice versa. Thus, thermoelectric materials are widely used for cooling and power generation applications. Indeed, thermoelectric materials could revolutionize power generation and cooling applications and have a huge impact on the environment. This is because thermoelectric materials do not use any harmful refrigerants for cooling, and they can generate electricity from industrial waste heat. But large scale commercial application of thermoelectric materials is limited by their hitherto low figures of merit around 1.0.

[0005] The efficiency of a thermoelectric material is typically measured or characterized by the thermoelectric figure of merit (Z), which is defined as the square of its Seebeck coefficient (S) times its electrical conductivity ( $\sigma$ , sigma) divided by its

thermal conductivity ( $\kappa$ , kappa) or  $Z=S^2\sigma/\kappa$ . The figure of merit  $Z$  generally depends on the macroscopic transport parameters of the materials, thus, a large figure of merit is provided by a thermoelectric material having a large Seebeck coefficient, high electrical conductivity, and low thermal conductivity. The product of the Seebeck coefficient ( $S$ ) squared and electrical conductivity ( $\sigma$ ), *i.e.*,  $\sigma S^2$ , is called thermopower. The higher the thermopower is for a material, the higher the thermoelectric efficiency of that material will be.

[0006] Because  $Z$  varies with temperature, a useful dimensionless figure of merit ( $ZT$ ) is often used as a measure of performance of a thermoelectric material. The dimensionless figure of merit is defined as  $ZT = [S^2\sigma/\kappa] * T$  where  $T$  is the average temperature. Generally, a greater  $ZT$  indicates a greater thermodynamic efficiency. Hence, a good thermoelectric material generally has a large Seebeck coefficient and good electrical conductivity with low thermal conductivity.

[0007] By way of further background, the Peltier effect is a measure of the "thermoelectric pumping power", which is the amount of heat that a material can pump per unit of electrical current. The Seebeck coefficient is further defined as the ratio of the open-circuit voltage ( $V$ ) to the temperature difference ( $T_H - T_C$ ) between the hot and cold junctions of a circuit exhibiting the Seebeck effect, or  $S=V/(T_H - T_C)$ . The electrical conductivity is a measure of a material's ability to conduct electrical current. The thermal conductivity is a measure of heat that is lost as it flows back against the heat pumped by a material.

[0008] Thermoelectric materials are commonly used in thermoelectric modules. A thermoelectric module (TEM) is a relatively small solid state device that can operate as a heat pump or as an electrical power generator. When a thermoelectric module is used as a heat pump, the thermoelectric module utilizes the Peltier effect to move heat and may then be referred to as a thermoelectric cooler (TEC) as shown in FIG. 1. When a thermoelectric module is used to generate electricity, the thermoelectric module may be referred to as a thermoelectric generator (TEG). The TEG may be electrically connected to a power storage circuit, such as a battery charger, *etc.* for storing electricity generated by the TEG.

[0009] With regard to use of a thermoelectric module as a TEC as shown in FIG. 1, the Peltier effect refers to the transport of heat that occurs when electrical current passes through a thermoelectric material. Heat is either picked up where electrons enter the material and is deposited where electrons exit the material (as is the case in an N-type thermoelectric material), or heat is deposited where electrons enter the material and is picked up where electrons exit the material (as is the case in a P-type thermoelectric material). A TEC is usually constructed by connecting alternating N-type and P-type elements of thermoelectric material ("elements") electrically in series and thermally in parallel. The use of an alternating arrangement of N-type and P-type elements causes electricity to flow in one spatial direction in all N-type elements and in the opposite spatial direction in all P-type elements. As a result, when connected to a direct current power source, electrical current causes heat to move from one side of the TEC to the other {e.g., from one circuit board to the other circuit board, etc.}. Naturally, this warms one side of the TEC and cools the other side. A typical application exposes the cooler side of the TEC to an object, substance, or environment to be cooled as shown in FIG. 1.

### SUMMARY

[0010] This section provides a general summary of the disclosure, and is not a comprehensive disclosure of its full scope or all of its features.

[001 1] According to various aspects, exemplary embodiments are disclosed of Bismuth Antimony Telluride (BiSbTe) based nano-bulk composites having high dimensionless figures of merit (ZT) and with nanostructured BiSbTe as the matrix (host) and bulk BiSbTe as the inclusion (guest). In an exemplary embodiment of a thermoelectric nano-bulk composite material, there is a matrix including nanostructured bismuth antimony telluride. The thermoelectric nano-bulk composite material also includes bulk bismuth antimony telluride in the matrix. A weight percentage ratio of the nanostructured bismuth antimony telluride to the bulk bismuth antimony telluride is at least one to one or higher.

[0012] Also disclosed are methods of making thermoelectric nano-bulk composite materials. In an exemplary embodiment, a method generally includes

incorporating bulk bismuth antimony telluride into a matrix including nanostructured bismuth antimony telluride, such that a weight percentage ratio of the nanostructured bismuth antimony telluride to the bulk bismuth antimony telluride is at least one to one or higher.

**[0013]** Further areas of applicability will become apparent from the description provided herein. The description and specific examples in this summary are intended for purposes of illustration only and are not intended to limit the scope of the present disclosure.

## DRAWINGS

[0014] The drawings described herein are for illustrative purposes only of selected embodiments and not all possible implementations, and are not intended to limit the scope of the present disclosure.

[0015] FIG. 1 is a schematic illustration showing an example thermoelectric module (TEM), specifically a thermoelectric cooler (TEC) having P-type and N-type thermoelectric materials where the P-type thermoelectric material may comprise a nanostructured sheet of bismuth antimony telluride nanoparticles or nano-bulk composite according to exemplary embodiments of the present technology.

[0018] FIG. 2 is a low magnification scanning electron microscope image of hot pressed bismuth antimony telluride nanoparticles that may be used as a matrix in a nano-bulk composite according to exemplary embodiments of the present technology.

[0017] FIGS. 3A and 3B are low and high magnification scanning electron microscope images of hot pressed nano-bulk composite including a matrix of bismuth antimony telluride nanostructured sheets and powdered bulk bismuth antimony telluride inclusion according to exemplary embodiments of the present technology.

[0018] FIG. 4 shows an XRD (X-ray diffraction) pattern or diffractogram plotted on a graph showing intensity in arbitrary units (a.u.) versus twice the angle of diffraction ( $2\theta$ ) in degrees for a hot pressed sample of a nano-bulk composite according to exemplary embodiments of the present technology.

[0019] FIG. 5 is a line graph of Seebeck coefficient versus temperature for a nano-bulk composite with a nano to bulk ratio of 70:30 according to exemplary embodiments of the present technology.

[0020] FIG. 6 includes lines graphs showing electrical conductivity (EC), thermal conductivity (TC), Seebeck coefficient (SC) and ZT recorded at room temperature for nano-bulk composites having a matrix that includes as prepared nanoparticles and a bulk powder inclusion in the matrix according to exemplary embodiments of the present technology.

[0021] FIGS. 7A and 7B are scanning electron microscope images of bismuth antimony telluride nanopowder as prepared prior to hot pressing according to exemplary embodiments of the present technology.

[0022] FIGS. 8A and 8B are scanning electron microscope images showing the nanostructured sheet formation after hot pressing bismuth antimony telluride nanopowder according to exemplary embodiments of the present technology.

[0023] FIGS. 9A and 9B are scanning electron microscope images showing formation of 2D sheet nanostructure in the hot pressed P-type pellets according to exemplary embodiments of the present technology.

[0024] FIG. 10 shows XRD (X-ray diffraction) patterns or diffractograms plotted on a graph showing intensity in arbitrary units (a.u.) versus twice the angle of diffraction ( $2\theta$ ) in degrees for bismuth antimony telluride nanopowder as prepared prior to hot pressing (powder sample a) and for hot pressed bismuth antimony telluride nanopowder (hot pressed sample b) according to exemplary embodiments of the present technology.

[0025] FIG. 11 is a line graph of Seebeck coefficient versus temperature obtained from hot pressed nanostructured bismuth antimony telluride according to exemplary embodiments of the present technology.

[0026] Corresponding reference numerals indicate corresponding parts throughout the several views of the drawings.

## DETAILED DESCRIPTION

[0027] Example embodiments will now be described more fully with reference to the accompanying drawings.

[0028] Thermoelectric materials with high ZT is desired for the replacement of compressor based refrigeration or meaningful power generation application in commercial scale. But the inventors recognized that increasing ZT is challenging because thermal conductivity  $\kappa$ , Seebeck coefficient  $a$ , electrical conductivity  $\sigma$ , follow opposing trends. Bismuth telluride based thermoelectric materials are considered as one of the best room temperature thermoelectric materials, commonly used for cooling application. But despite prior efforts, ZT of bismuth telluride based materials at room temperature remains at 0.8 to 0.9.

[0029] The inventors hereof recognized that ZT for thermoelectric composite materials based on Bismuth Antimony Telluride (BiSbTe) may be enhanced by decreasing thermal conductivity through interfacial phonon scattering, while at the same time increasing the density of states near Fermi level in the nanostructure present in the composite to enhance Seebeck coefficient. The inventors also recognized that the presence of bulk in a composite will provide better connectivity between nanostructures, which will help in retention of good electrical conductivity.

[0030] After recognizing the above, the inventors developed and disclose herein exemplary embodiments of BiSbTe based nano-bulk composites having enhanced or high dimensionless figures of merit (ZT). In exemplary embodiments, the nano-bulk composite comprises nanostructured BiSbTe {e.g., nanoparticles, sheets, platelets, other nanostructures, etc.) as the matrix (host) and BiSbTe bulk as the inclusion (guest) in the matrix. This is unlike existing composites in which the matrix/host is bulk material and nanoparticles are the filler or inclusion. Accordingly, an exemplary embodiment of a nano-bulk composite may also be referred to herein as a reverse composite due to the reversed roles of using nanostructured BiSbTe as the matrix (host) and BiSbTe bulk as the inclusion (guest).

[0031] The nanostructured bismuth antimony telluride {e.g., nanoparticles, sheets, platelets, other nanostructures, etc.) used as the matrix (host) may be made, prepared, or synthesized in various ways. For example, the matrix may comprise 2D

nanostructured sheets of bismuth antimony telluride as disclosed hereinafter and/or made by an exemplary method disclosed herein {e.g., via synthesizing nanoparticles via wet chemistry using salts of tellurium and antimony with bismuth powder and 1,5-pentanediol or ethylene glycol solvents, etc.}. Accordingly, a nano-bulk composite may include 2D nanostructured sheets of bismuth antimony telluride as the matrix (host) in exemplary embodiments. By way of example, a nano-bulk composite may include nanostructured bismuth antimony telluride comprising a P-type material with a composition of  $\text{Bi}_{40-x}\text{SbxTe}_{60}$ , where  $x = 25$  to  $32$ . In one particular example, the nano-bulk composite includes a matrix comprising P-type bismuth antimony telluride nanoparticles with a composition of  $\text{Bi}_{0.4}\text{Sbi.6Te}_3$ . Alternative embodiments may include other bismuth antimony telluride nanostructures for the matrix (host), such as other sheet nanostructures, nanoparticles (e.g., as prepared nanoparticles, etc.), platelets, bismuth antimony telluride having a different composition, etc.

[0032] By way of example, the bulk bismuth antimony telluride may be prepared from constituent metals, viz., bismuth, antimony, and tellurium by a melting route. Zone melting may be carried out to obtain single crystal bismuth antimony telluride material. The single crystal material may be crushed to obtain bulk powder.

[0033] Also by way of example, the matrix may comprise nanostructures of bismuth antimony telluride {e.g.,  $\text{Bi}_{40-x}\text{SbxTe}_{60}$ , where  $x = 25$  to  $32$ ) that are synthesized by a wet chemical method as disclosed in more detail below. For example, salts/compounds of tellurium and antimony along with bismuth powder/salts may be reacted in ethylene glycol with reaction temperatures in the range of  $110\text{ }^\circ\text{C}$  to  $180\text{ }^\circ\text{C}$ . Hydrazine hydrate may be used as the reducing agent. The obtained nanoparticles may be purified by repeated centrifuging and washing with water and finally dried under vacuum. See, for example, FIGS. 7A and 7B which are scanning electron microscope images of bismuth antimony telluride nanopowder as prepared prior to hot pressing or mixing with a bulk powder.

[0034] In exemplary embodiments, a nano-bulk composite comprises a matrix of as prepared nanoparticles into which is mixed bulk bismuth antimony telluride powders in different weight percentage ratios, such as 50:50, 55:45, 60:40, 65:35, 70:30, 75:25, 80:20, 85:15, 90:10, 95:5, etc. where the first number indicates the weight



percentage of the matrix of as prepared nanoparticles and the second number indicates the weight percentage of the bulk material inclusion. Pestle and mortar may be used to thoroughly mix the mixture of as prepared nanoparticles and bulk material. Hot pressing of the composite powder may then be carried out, *e.g.*, within a temperature range of 300 °C to 500 °C and at a force of 150 kilograms per centimeter squared ( $\text{kg}/\text{cm}^2$ ) to 400  $\text{kg}/\text{cm}^2$  for a duration of between 2 hours to 4 hours. This hot pressing of nanoparticles results in a dense pellet whose theoretical density varies from 94% to 97%.

[0035J Table 1 below provides transport properties at room temperature (about 300 Kelvin) for nano-bulk composites including a matrix of as prepared bismuth antimony telluride nanoparticles and bismuth antimony telluride bulk commercial powder, where the samples included different weight percentages of the as prepared nanoparticle matrix to the bulk powder inclusion. For example, sample 3 included 60% by weight of the as prepared nanoparticles and 40% by weight of the bulk powder. For comparison purposes, Table 1 also includes thermoelectric properties for the as prepared nanoparticles (sample 1) and for the bulk powder (sample 2).

[0036J Table 1 below provides electrical conductivity (in Siemens per centimeter ( $\text{S}/\text{cm}$ )), thermal conductivity (in Watts per meter Kelvin ( $\text{W}/\text{mK}$ )), Seebeck coefficient (in microvolts per Kelvin ( $\mu\text{V}/\text{K}$ )), and ZT at room temperature for these six samples. Thermal conductivity was measured by hot disk. Electrical conductivity was measured via a Jandel four probe technique. Seebeck coefficient was measured using MMR (Micro Miniature Refrigerators) Seebeck instrument. These samples and numerical values set forth in Table 1 below are merely examples, as other exemplary embodiments of a nano-bulk composite may include different weight percentages of the as prepared nanoparticles to the bulk powder (*e.g.*, 50:50, 55:45, 65:35, 75:25, 95:5, *etc.*) and/or different (*i.e.*, higher or lower) Seebeck coefficient, ZT, thermal conductivity, and/or electrical conductivity.

**[0037] TABLE 1**

Sample type	Composition Nano:Bulk	Electrical conductivity (S/cm) ( $\sigma$ )	Power factor ( $\mu\text{W}/\text{cmK}^2$ ) ( $S^2 \cdot \sigma$ )	Thermal conductivity (W/mK) ( $\kappa$ )	Seebeck coefficient ( $\mu\text{V}/\text{K}$ ) (S)	ZT
1	100: 0	338	32.27	0.86	309	1.14
2	0: 100	1094	42.46	1.12	197	1.14
3	60:40	690	39.74	0.95	240	1.26
4	70:30	629	40.26	0.91	253	1.33
5	80:20	615	40.62	0.87	257	1.40
6	90:10	511	37.25	0.80	270	1.39

[0038] As shown in table 1 above, each sample nano-bulk composite had a higher room temperature ZT than the as prepared nanoparticles (sample 1) and the bulk powder (sample 2) under similar processing conditions. These sample nano-bulk composites had a Seebeck coefficient within a range of 240  $\mu\text{V}/\text{K}$  to 270  $\mu\text{V}/\text{K}$ , a ZT at room temperature within a range from 1.26 to 1.40, a thermal conductivity within a range from 0.80 W/mK to .95 W/mK, and an electrical conductivity within a range from 511 S/cm to 690 S/cm. This test data (which is also plotted in FIG. 6) reveals that the nano-bulk composites have enhanced ZT by increasing the power factor, decreasing thermal conductivity through interfacial phonon scattering, while at the same time increasing the density of states near Fermi level in the nanostructure present in the composite to enhance Seebeck coefficient. The presence of the bulk in the composite also provides better connectivity between nanostructures, which helps in retention of good electrical conductivity. Opposing trends between thermal conductivity  $\kappa$ , electrical conductivity  $\sigma$  and Seebeck coefficient  $a$  have been minimized or at least reduced. See also FIG. 5 showing the temperature dependent Seebeck coefficient of a nano-bulk composite with nano to bulk ratio of 70:30. In addition, FIG. 6 includes line graphs showing electrical conductivity (EC), thermal conductivity (TC), Seebeck coefficient (SC) and ZT recorded at room temperature (about 300 Kelvin) for nano-bulk composites having a matrix of as prepared nanoparticles and bulk powder inclusion according to exemplary embodiments of the present technology. The test data for samples 3 through 6 is also included in these line graphs. With the decrease in the weight percent of bulk

BiSbTe, the Seebeck coefficient increases and thermal conductivity decreases. At higher weight percent of bulk, the power factor increase is due to contribution from electrical conductivity and at lower weight percent of bulk the thermal conductivity contributes to enhance power factor.

[0039] As just described, exemplary embodiments of a nano-bulk composite may comprise a matrix of as prepared nanoparticles into which is mixed bulk bismuth antimony telluride powders. In other exemplary embodiments, the nano-bulk composite comprises a matrix of crushed, hot-pressed bismuth antimony telluride nanopowder into which is mixed bulk bismuth antimony telluride powders in different weight percentage ratios, such as 50:50, 55:45, 60:40, 65:35, 70:30, 75:25, 80:20, 85:15, 90:10, 95:5, *etc.* where the first number indicates the weight percentage of the nanopowder matrix and the second number indicates the weight percentage of the bulk material inclusion.

[0040] In these exemplary embodiments, the nanopowder may be formed by hot pressing as prepared bismuth antimony telluride nanoparticles and then crushing the hot pressed nanoparticles. For example, dried nanoparticles may be placed in graphite die and pressed under vacuum to obtain a compact pellet. The hot pressing of dried nanoparticles may be carried out, *e.g.*, within a temperature range of 300 °C to 500 °C and at a force of 150 kg/cm<sup>2</sup> to 400 kg/cm<sup>2</sup> for a duration of between 2 hours to 4 hours. See, for example, FIG. 2 which is a low magnification scanning electron microscope image showing the nanostructured sheet formation of the hot pressed bismuth antimony telluride nanoparticles. The obtained hot pressed pellet may be crushed into a nanopowder.

[0041] Pestle and mortar may be used to thoroughly mix the mixture of nanopowder and bulk powder. Hot pressing of the nano-bulk composite comprising the nanopowder matrix and the bulk powder inclusion may then be carried out, *e.g.*, within a temperature range of 300 °C to 500 °C and at a force of 150 kg/cm<sup>2</sup> to 400 kg/cm<sup>2</sup> for a duration of between 2 hours to 4 hours. See, for example, FIGS. 3A and 3B which are low and high magnification scanning electron microscope images of hot pressed nano-bulk composite including a matrix of bismuth antimony telluride nanostructured sheets and bulk bismuth antimony telluride bulk powder. The SEM images of FIGS. 3A and 3B show nanostructured sheets with dimensions in the range of 50 to 150 nanometers (nm)

and that the nanostructured sheets of BiSbTe are in intimate contact with the bulk particle, thereby decreasing the long range order seen in the case of nanoparticles alone. Hot pressing of the nanostructured BiSbTe in the presence of the bulk BiSbTe perturbs the order of the sheet structure, which results in highly randomized short range sheet structures being formed. See also FIG. 4, which includes an XRD pattern or diffractogram for a hot pressed sample of a nano-bulk composite that shows pure bismuth antimony telluride phase.

**[0042]** Table 2 below provides transport properties at room temperature (about 300 Kelvin) for nano-bulk composites including a matrix of bismuth antimony telluride nanopowder (crushed hot pressed nanoparticles) and bulk bismuth antimony telluride powder, where the three samples included different weight percentages of the nanopowder matrix to the bulk powder inclusion. For example, sample 2 included 60% by weight of the nanopowder and 40% by weight of the bulk powder. Thermal conductivity was measured by hot disk. Electrical conductivity was measured using by Jandel four probe technique. Seebeck coefficient was measured using MMR (Micro Miniature Refrigerators) Seebeck instrument. These samples and numerical values set forth in Table 2 below are merely examples, as other exemplary embodiments of a nano-bulk composite may include different weight percentages of the nanopowder to the bulk powder (*e.g.*, 55:45, 65:35, 70:30, 75:25, 80:20, 85:15, 95:5, *etc.*) and/or different (*i.e.*, higher or lower) Seebeck coefficient, ZT, thermal conductivity, and/or electrical conductivity.

**[0043] TABLE 2**

Sample type	Composition Nano:Bulk	Electrical conductivity (S/cm) ( $\sigma$ )	Power factor ( $\mu\text{W}/\text{cmK}^2$ ) ( $S^{2*}\sigma$ )	Thermal conductivity (W/mK) ( $\kappa$ )	Seebeck coefficient ( $\mu\text{V}/\text{K}$ ) (S)	ZT
1	50:50	823	45.84	0.99	236	1.39
2	60:40	727	46.17	0.98	252	1.41
3	90:10	600	44.72	0.89	273	1.51

**[0044]** As shown in Table 2 above, each sample of nano-bulk composite had a higher room temperature ZT than as prepared nanoparticles (ZT of 1.14, sample 1 in

table 1) and bulk powder (ZT of 1.14, sample 2 in table 1) under similar processing conditions. The sample nano-bulk composites, including a matrix of nanopowder (crushed, hot-pressed as prepared nanoparticles) and bulk powder inclusion, had a Seebeck coefficient within a range of 236  $\mu\text{V}/\text{K}$  to 273  $\mu\text{V}/\text{K}$ , a ZT at room temperature within a range from 1.39 to 1.51, a thermal conductivity within a range from 0.89 W/mK to 0.99 W/mK, and an electrical conductivity within a range from 600 S/cm to 823 S/cm. This test data reveals that the nano-bulk composites have enhanced ZT by increasing the power factor, decreasing thermal conductivity through interfacial phonon scattering, while at the same time increasing the density of states near Fermi level in the nanostructure present in the composite to enhance Seebeck coefficient. The presence of the bulk in the composite also provides better connectivity between nanostructures, which helps in retention of good electrical conductivity. Opposing trends between thermal conductivity  $\kappa$ , electrical conductivity  $\sigma$  and Seebeck coefficient  $a$  have been minimized or at least reduced. ZT approaches maximum with nano to bulk ratio of 90:10, which indicates that a small amount of bulk is sufficient to raise power factor in a reverse nano-bulk composite.

[0045J] As shown by Tables 1 and 2 and depending on the composition of the nano-bulk composite samples, the room temperature thermal conductivity ranges from 0.80 to 0.99 W/mK, the room temperature electrical conductivity ranges from 511 to 823 S/cm, the room temperature Seebeck coefficient ranges from 236  $\mu\text{V}/\text{K}$  to 273  $\mu\text{V}/\text{K}$ , and the room temperature ZT ranges from 1.26 to 1.51. By way of comparison, the thermoelectric transport properties of pure nanoparticles may have a room temperature thermal conductivity of 0.86 to 0.89 W/mK, room temperature electrical conductivity of 290 to 354 S/cm, and room temperature Seebeck coefficient of 290 to 310  $\mu\text{V}/\text{K}$ .

[0046] The exemplary embodiments of nano-bulk composites disclosed herein have a reported very high ZT compared to the reported value of ZT for conventional bulk and reported composite thermoelectric materials. ZT of P-type materials at room temperature is in the range 0.5 to 1.1, while the nano-bulk composite materials disclosed herein have room temperature ZT from 1.26 to 1.51 depending on the nano to bulk ratio. In contrast to some existing thermoelectric materials having only 15 weight percent of nanoparticles, exemplary embodiments disclosed herein have at

least 50 weight percentage (e.g., 50 to 90 weight percentage) of nanoparticles with remainder being bulk material. Accordingly, some exemplary embodiments disclosed herein have a greater weight percentage of nanoparticles than the weight percentage of the bulk material. The inventors have found that the addition of more nanoparticles may lead to 10 to 20% reduction of thermal conductivity and in turn increased ZT.

[0047] Accordingly, the inventors hereof have disclosed exemplary embodiments of nano-bulk bismuth antimony telluride thermoelectric materials and methods of making the same that may provide one or more (but not necessarily any or all) of the following advantages. For example, nano-bulk composite P-type bismuth antimony telluride thermoelectric materials have better compressive or mechanical strength compared to conventional bulk bismuth antimony telluride. Better compressive strength will help reduce wear and damage in harsh conditions. Thus, during cutting of p-legs to make a thermoelectric module, the disclosed nano-bulk composite materials will produce high yields compared to conventional bulk materials. ZT is enhanced by increasing power factor. Opposing trends between thermal conductivity  $\kappa$ , electrical conductivity  $\sigma$ , and Seebeck coefficient  $S$  have been minimized or at least reduced. ZT has been increased, e.g., by 20% to 50% in the nano-bulk composites as compared to the ZT of parent nano and/or parent bulk bismuth antimony telluride. This indicates that the nano-bulk composite route disclosed herein can enhance ZT for a nano-bulk composite disclosed herein where nanomaterial is used as the matrix (host) and bulk (e.g., microparticles, micron-sized particles, etc.) are used as the inclusion (guest). Presence of bulk in the nanomatrix leads to formation of randomized short range sheet nanostructure in the nano-bulk composite. This results in very low thermal conductivity limiting towards thermal conductivity of pure nano. ZT approaches maximum with nano to bulk ratio (90:10). This indicates that in a reverse nano-bulk composite, a small amount of bulk is sufficient to raise power factor. The methods of making BiSbTe based nano-bulk composites are highly repeatable, reproducible, reliable, and cost effective.

[0048] In addition, the inventors hereof have further recognized that nanostructuring is one of the best strategies to enhance ZT by decreasing thermal conductivity through interfacial phonon scattering and increasing Seebeck coefficient due to increased density of states near Fermi level. Accordingly, the inventors hereof

have developed and disclose herein exemplary embodiments of nanostructured bismuth antimony telluride thermoelectric materials having a high ZT {e.g., 0.78, 1.16, 1.39, 1.7, 2, greater than 2, etc.) at room temperature. The nanostructured bismuth antimony telluride thermoelectric materials may comprise P-type materials with a composition of  $\text{Bi}_{40-x}\text{Sb}_x\text{Te}_{60}$ , where  $x = 25$  to  $32$ . An exemplary embodiment includes nanoparticles of bismuth antimony telluride having a composition of  $\text{Bi}_{30}\text{Sb}_{30}\text{Te}_{60}$ , and accordingly  $x$  is  $30$  in the composition of  $\text{Bi}_{40-x}\text{Sb}_x\text{Te}_{60}$ . In other exemplary embodiments,  $x$  may be a different value greater than or less than  $30$ , e.g., within the range of  $25$  to  $32$ . Any one or more of the exemplary embodiments of nanostructured bismuth antimony telluride thermoelectric materials disclosed herein may be used as a matrix in a nano-bulk composite. But a nanostructured bismuth antimony telluride thermoelectric material may also be used as a thermoelectric P-type material or in other applications.

[0049] The inventors have also disclosed herein exemplary methods of making nanostructured bismuth antimony telluride thermoelectric materials {e.g., synthesizing nanoparticles via wet chemistry using salts of tellurium and antimony with bismuth powder/ $\text{BiCl}_3$  and 1,5-pentanediol or ethylene glycol solvents, etc.). In exemplary embodiments, nanoparticles of bismuth antimony telluride {e.g.,  $\text{Bi}_{40-x}\text{Sb}_x\text{Te}_{60}$ , where  $x = 25$  to  $32$ , etc.) are synthesized by chemical route, which is amenable for large scale synthesis. As disclosed herein, bismuth powder is used as a starting material instead of bismuth salts for the preparation of the nanostructured bismuth antimony telluride thermoelectric materials by wet chemical route.

[0050] Salts of tellurium and antimony along with bismuth powder/ $\text{BiCl}_3$  may be reacted in ethylene glycol, 1,5-pentanediol, or any diol. The reaction temperatures may be in the range from  $110^\circ\text{C}$  to  $180^\circ\text{C}$  for ethylene glycol reaction and  $110^\circ\text{C}$  to  $240^\circ\text{C}$  for 1,5-pentanediol reaction. Other embodiments may include using propane diol, butane diol, pentanediol, other diols, etc. Hydrazine hydrate may be used as a reducing agent. The obtained nanoparticles {e.g.,  $\text{Bi}_{30}\text{Sb}_{30}\text{Te}_{60}$  nanoparticles, etc.) may then be cleaned by repeated centrifugation and washing with water. The nanoparticles may be dried under vacuum and subject to densification by vacuum hot press. Accordingly, the inventors have developed and disclose herein scalable technology for obtaining high ZT nanostructured bismuth antimony telluride, which technology includes

synthesis by chemical route using bismuth powder as a starting material and densification by vacuum hot press.

**[0051]** As just noted, the inventors' have developed and disclosed herein bismuth antimony telluride ( $\text{Bi}_{4_0-x}\text{Sb}_x\text{Te}_6_0$  where  $x = 25 - 32$ ) nanoparticles that are synthesized by a wet-chemical route using 1,5-pentanediol, ethylene glycol, other diol, *etc.* A description will now be provided for synthesizing nanoparticles of bismuth antimony telluride via both the 1,5-pentanediol route and for the ethylene glycol route. These specific examples are provided for purposes of illustration, as other methods may also be used.

**[0052]** For the 1,5-pentanediol route, the synthesis of BiSbTe nanopowder includes dissolving telluric acid (*e.g.*, 179.08 millimoles (mmol) to 358 mmol, *etc.*) and antimony acetate (*e.g.*, 89.56 mmol to 180 mmol, *etc.*) in 350 milliliters (ml) to 700 ml of 1,5-pentanediol (reaction mixture A) at about 100 °C. In a separate beaker or other container, bismuth metal powder (*e.g.*, 29.83 mmol to 60.0 mmol, *etc.*) is dissolved in 10 ml to 15 ml concentrated nitric acid (reaction mixture B). The reaction mixture B is then transferred to or combined with reaction mixture A. The reducing agent hydrazine hydrate (99% solution) is added to the combined reaction mixtures A and B containing the constituent components. The temperature of the combined reaction mixtures and reducing agent is then raised to a temperature between about 110 °C to about 240 °C, and the reaction is continued under constant stirring for a duration of 1 hour to 6 hours to allow the complete alloy formation. As noted above, the obtained nanoparticle powder may then be cleaned by repeated centrifugation and washing with water, and thereafter dried under vacuum. Accordingly, this exemplary method includes the synthesis of the BiSbTe by a bottom up route starting with bismuth metal powder. Advantageously, bismuth metal powder is non-hazardous while other bismuth salts are hazardous.

**[0053]** For the ethylene glycol route, the synthesis of BiSbTe nanopowder includes dissolving telluric acid (*e.g.*, 114.6 mmol to 230 mmol, *etc.*) and antimony acetate (*e.g.*, 58.2 mmol to 119 mmol, *etc.*) in 300 ml to 500 ml ethylene glycol (reaction mixture A) at 80 °C to 100 °C. In a separate beaker or other container, bismuth metal powder (*e.g.*, 19.4 mmol to 40 mmol, *etc.*) is dissolved in 5 ml to 8 ml concentrated



Nitric acid (reaction mixture B). The reaction mixture B is then transferred to or combined with reaction mixture A. The reducing agent, hydrazine hydrate, is added to the combined reaction mixtures A and B containing constituent components. The temperature of the combined reaction mixtures is then raised to a temperature between about 110 °C to about 180 °C, and the reaction is continued under constant stirring for a duration of 20 hours to 48 hours to allow the complete alloy formation. The obtained nanoparticle powder may then be cleaned by repeated centrifugation and washing with water, and thereafter dried under vacuum. Accordingly, this exemplary method also includes the synthesis of the BiSbTe by a bottom up route starting with bismuth metal powder. Advantageously, bismuth metal powder is non-hazardous while other bismuth salts are hazardous.

[0054] The dried bismuth antimony telluride nanopowder may next undergo surface treatment or controlled oxidation. In this process, the dried nanoparticles of bismuth antimony telluride {e.g., 14 grams, etc.) may be placed in a three neck round bottom flask and purged with argon gas containing a H<sub>2</sub>O and O<sub>2</sub> of the order of 20 parts per million (ppm) to 100 ppm. The nanoparticles of bismuth antimony telluride may be exposed to argon gas that flows over a bed of nanoparticles for a period of 1 hour to 6 hours. The surface treated nanopowders may thereafter be processed further in vacuum hot press as explained herein.

[0055] By way of example only, the inventors have recognized that as prepared bismuth antimony telluride nanopowder having a very high electrical conductivity {e.g., 1500 Siemens per centimeter (S/cm) to 1850 S/cm, etc.), a low Seebeck coefficient, and high thermal conductivity will consequently have a low/poor room temperature ZT prior to surface treatment. The inventors have also discovered that surface treatment and sintering results in surface oxidation for that same powder, which, in turn, causes a decrease in electrical conductivity and an increase in Seebeck coefficient that helps augment or enhance ZT. Accordingly, some exemplary embodiments include surface treating nanoparticles of bismuth antimony telluride having a high electrical conductivity and then hot pressing the surface treated nanoparticles of bismuth antimony telluride. The surface treatment helps to improve or enhance the ZT of the resulting nanostructured bismuth antimony telluride as compared

to as prepared bismuth antimony telluride nanopowder having a very high electrical conductivity that is hot pressed without any surface treatment. This is shown below by a comparison of Sample 1 which has a  $ZT = 0.34$  with Sample 2 which has a  $ZT = 2.0$ . As explained below, Sample 1 was prepared by hot pressing bismuth antimony telluride nanopowder having a very high electrical conductivity without surface treatment. Sample 2 was prepared by hot pressing the same batch bismuth antimony telluride nanopowder post surface treatment.

**[0056]** As also explained below, the inventors have also discovered that surface treatment and controlled oxidation doesn't help to increase  $ZT$  for as prepared bismuth antimony telluride nanopowder having a low electrical conductivity {e.g., 400 S/cm to 800 S/cm, etc.}. This is shown below by a comparison of Sample 3 ( $ZT = 1.7$ ) and Sample 4 ( $ZT = 1.39$ ) with Sample 5 ( $ZT = 1.16$ ) and Sample 6 ( $ZT = .78$ ). As explained below, Samples 3 and 4 were prepared by direct hot pressing of as prepared bismuth antimony telluride nanopowder without surface treatment. Samples 5 and 6 were prepared by hot pressing the same batch bismuth antimony telluride nanopowder but the hot pressing was carried out after surface treatment. Accordingly, some exemplary embodiments include hot pressing nanoparticles of bismuth antimony telluride having a low electrical conductivity without surface treating the nanoparticles prior to the hot pressing.

**[0057]** In regard to powder characterization, the morphology and composition of the nanoparticles may be characterized by Scanning Electron Microscopy (SEM) and Energy Dispersive X-ray spectroscopy (EDS). XRD (X-ray diffraction) may be used to check phase purity of the nanoparticles. For example, FIGS. 7A and 7B are SEM images of bismuth antimony telluride nanopowder as prepared prior to hot pressing. FIG. 10 includes XRD patterns or diffractograms for bismuth antimony telluride nanopowder as prepared prior to hot pressing (see powder sample a) and for hot pressed bismuth antimony telluride nanopowder (see hot pressed sample b). FIG. 10 generally shows pure bismuth antimony telluride phase.

**[0058]** In exemplary embodiments, dried nanoparticles {e.g., around 15 grams, etc.} may be hot pressed using graphite dies. The hot pressing may be performed under a vacuum atmosphere with the following conditions. The temperature

may be from about 300 °C to about 500 °C. The pressure may be from about 150 kilograms per square centimeter ( $\text{kg/cm}^2$ ) to about 400  $\text{kg/cm}^2$ . The duration of the hot pressing may last between about 2 hours to about 4 hours.

[0059] In an exemplary embodiment, dried nanoparticles may be hot pressed at a temperature from about 300 °C to about 500 °C and a pressure from about 150  $\text{kg/cm}^2$  to about 400  $\text{kg/cm}^2$ . This exemplary embodiment includes unique hot pressing parameters, such as very slow heating and cooling rates in combination with slow increases in pressure or force rate to help obtain a 2D sheet structure. For example, the pressure may be increased at the rate of about 15  $\text{kg/cm}^2$  to about 20  $\text{kg/cm}^2$  per minute until the final pressure is reached, which may be from about 150  $\text{kg/cm}^2$  to about 400  $\text{kg/cm}^2$ . A very slow cooling rate (e.g., active cooling, etc.) may be used to bring the sample to room temperature to help avoid development of stress inside the sample. In an exemplary embodiment, cooling was controlled with a cooling rate of 2 degrees per minute with continuous water circulation.

[0060] In regard to the characterization of sintered materials, samples obtained may have a density of more than 95% of theoretical density in an exemplary embodiment. The thicknesses of the sheets may vary, such as from 30 nm to 50 nm, etc. FIGS. 8A and 8B are SEM images showing the nanostructured sheet formation after hot pressing bismuth antimony telluride nanopowder. FIGS. 9A and 9B are SEM images showing the organization of the sheet structure that results in the formation of a 2D sheet nanostructure in the hot pressed P-type pellets. Generally, these figures show retention of the nanostructure after hot pressing.

[0061] By way of background, spark plasma sintering (SPS) may be used for the retention of nanostructure in post sintered samples. Because SPS is a very fast process, the chance of retaining the nanostructure is high. But the inventors hereof have been able to retain a 2D sheet nanostructure despite having a sample under elevated temperature and pressure for a relatively long time during vacuum hot pressing (e.g., about 2 hours to about 4 hours in duration, etc.).

[0062] In exemplary embodiments, nanostructured bismuth antimony telluride nanoparticles are formed via hot pressing so as to have a microstructure comprising a 2D sheet structure, e.g., having a thickness dimension in the range of 30 to 50

nanometers, *etc.* In an exemplary embodiment, nanoparticles of  $\text{Bi}_{10}\text{Sb}_3\text{Te}_6\text{O}$  are hot pressed into a 2D sheet nanostructure having high ZT (*e.g.*, 2 or more, *etc.*) at room temperature. Without wishing to be bound to any particular theory, the inventors believe that the high values of ZT for P-type materials at room temperature are achievable or attributable to the inventors' unique microstructures (2D sheet nanostructures).

[0063] By way of background, the term "nanoparticles" as used herein may generally refer to particles whose size falls between 1 nanometer (nm) to 100 nm. A single crystal may generally refer to materials with a continuous crystal lattice with a very long range order (*e.g.*, single crystal silicon, *etc.*). Nanoparticles can be single crystals or amorphous depending on the lattice order. Nanoparticles with a single domain or defined grain may also be referred to as nanocrystals. A two-dimensional (2D) sheet nanostructure may generally refer to a nanostructure having length and width dimensions in the X and Y direction in micrometers ( $\mu\text{m}$ ) and a thickness dimension in the Z direction in nanometers (nm).

[0064] The inventors' have disclosed herein as prepared particles/flakes/platelets that may range in size from 20 nm to 100 nm, and thus may be referred to as nanocrystals. Also disclosed herein are methods that include hot pressing bismuth antimony telluride nanoparticles, which results in 2D sheet nanostructure having a thickness dimension (in the Z direction) in the nanometer range (*e.g.*, 30 nm to 50 nm, *etc.*) and length and width dimensions (in the X and Y directions) in the micrometer range. Accordingly, the inventors have disclosed bismuth antimony telluride nanoparticles that are nanocrystals as prepared (*e.g.*, see FIGS. 7A and 7B, *etc.*) and that are nanocrystals after being hot pressed into 2D sheet nanostructures (*e.g.*, FIG. 8A through FIG. 9B, *etc.*).

[0065] Six samples of nanostructured bismuth antimony telluride ( $\text{Bi}_{10}\text{Sb}_3\text{OTe}_6$ ) P-type thermoelectric materials were produced using exemplary methods of the present technology. Samples 1 and 2 were synthesized using 1,5-pentanediol. Samples 3, 4, 5, and 6 were synthesized using ethylene glycol. In addition, Samples 1, 3, and 4 were hot pressed without surface treatment. In contrast, Samples 2, 5, and 6 were oxidized in a controlled way by purging the nanopowder sample with a mixture of argon, oxygen, and moisture. Accordingly, Samples 1, 3, and 4 were hot pressed

without argon gas purging, while Samples 2, 5, and 6 were hot pressed after purging with argon gas. The composition was the same for all six samples  $\text{Bi}_0\text{Sb}_3\text{Te}_6$ .

[0086] Transport properties (thermal conductivity, electrical conductivity and Seebeck coefficient) of sintered pellets of Samples 1 through 6 were measured to evaluate ZT at room temperature of 300 degrees Kelvin. Thermal conductivity was measured using a hot disk TPS 2500S instrument. Electrical conductivity was measured using a Jandel RM3-AR four probe technique. Seebeck coefficient was measured using an MMR SB-100 instrument. Table 3 below provides the electrical conductivity (in Siemens per centimeter (S/cm)), thermal conductivity (in Watts per meter Kelvin (W/mK), Seebeck coefficient (in microvolts per Kelvin ( $\mu\text{V}/\text{K}$ )), and ZT for these six samples. These samples and numerical values set forth in Table 3 below are merely examples, as other exemplary embodiments may include nanostructured bismuth antimony telluride thermoelectric materials having a different, *i.e.*, higher or lower, Seebeck coefficient, ZT, thermal conductivity, and/or electrical conductivity.

**[0067] TABLE 3**

Sample ID	Electrical Conductivity (S/cm) ( $\sigma$ )	Thermal Conductivity (W/mK) ( $\kappa$ )	Seebeck Coefficient ( $\mu\text{V}/\text{K}$ ) (S)	ZT (at room temperature)
1	1823	1.2	86	0.34
2	882	1.0	276	2.0
3	533	0.76	293.4	1.7
4	413	0.86	311	1.39
5	354	0.87	308.5	1.16
6	264	0.89	297	0.78

[0068] As shown in Table 3 above for these exemplary embodiments, the nanostructured bismuth antimony telluride thermoelectric materials of Samples 2 through 6 have a Seebeck coefficient of at least 276  $\mu\text{V}/\text{K}$  and a ZT at room temperature of at least 0.78. Also shown in Table 3 above, these exemplary nanostructured bismuth antimony telluride thermoelectric materials of Samples 2

through 6 have a Seebeck coefficient within a range from 276  $\mu\text{v}/\text{K}$  to 311  $\mu\text{v}/\text{K}$ , a ZT at room temperature within a range from 0.78 to 2, a thermal conductivity within a range from 0.76 W/mK to 1.0 W/mK, and an electrical conductivity within a range from 264 S/cm to 882 S/cm.

[0069] Sample 1 which was hot pressed without surface treatment had a considerably higher electrical conductivity, lower Seebeck coefficient, and lower ZT than Sample 2, which was hot pressed after surface treatment of the same batch powder as that of Sample 1. More specifically, Sample 1 has a very high electrical conductivity of 1823 S/cm and low Seebeck coefficient of 86  $\mu\text{v}/\text{K}$ , which results in a poor ZT = 0.34. By comparison, Sample 2 has a lower electrical conductivity of 882 S/cm and higher Seebeck coefficient of 276  $\mu\text{v}/\text{K}$ , which results in an improved or enhanced ZT = 2.0. Thus, the surface treatment of Sample 2 prior to hot pressing helped to reduce electrical conductivity and increase Seebeck coefficient, which, in turn, drastically improved the ZT albeit at the expense of reduced electrical conductivity. For thermoelectric materials, a very high electrical conductivity results in a poor Seebeck coefficient. But as shown by the comparison of Sample 1 with Sample 2, surface treatment or controlled oxidation can reduce electrical conductivity and increase Seebeck coefficient, which results in an improved or enhanced ZT when the starting nanostructured bismuth antimony telluride powder has a very high electrical conductivity {e.g., 1500 S/cm to 1850 S/cm, etc.}.

[0070] The inventors have also discovered that surface treatment or controlled oxidation doesn't necessarily help to increase ZT for as prepared bismuth antimony telluride nanopowder having a low electrical conductivity {e.g., 400 S/cm to 800 S/cm, etc.}. This is shown by a comparison of Sample 4 (ZT = 1.39) and Sample 5 (ZT = 1.16). Sample 4 was prepared by hot pressing bismuth antimony telluride nanopowder without surface treatment. Sample 5 was prepared by hot pressing the same batch powder but the hot pressing was carried out after surface treatment. As shown by a comparison of Samples 4 and 5, the electrical conductivity decreased from 413 S/cm to 354 S/cm when surface treatment was performed prior to hot pressing. Accordingly, the extent of the reduction on electrical conductivity due to the surface treatment and oxidation was relatively minor or minimal when the as prepared sample has a low electrical conductivity {e.g., 400 S/cm to 800 S/cm, etc.}. In contrast, Samples

1 and 2 above show that a drastic reduction in electrical conductivity may occur when the as prepared starting sample has a very high electrical conductivity {e.g., 1500 S/cm to 1850 S/cm, etc.}.

[0071] When the as prepared powder has low electrical conductivity, controlled oxidation doesn't help to increase ZT. For example, Samples 3 and 4 had respective low electrical conductivities of 533 S/cm and 413 S/cm, which results in high Seebeck coefficients of 293.4  $\mu\text{V}/\text{K}$  and 311  $\mu\text{V}/\text{K}$  and ZT of 1.7 and 1.39. As shown by Samples 5 and 6 and their respective ZT of 1.16 and 0.78, surface treatment and further oxidation may reduce ZT when the as prepared bismuth antimony telluride nanopowder has a low electrical conductivity {e.g., 400 S/cm to 800 S/cm, etc.}.

[0072] FIG. 11 is a line graph of Seebeck coefficient versus temperature for nanostructured bismuth antimony telluride {e.g.,  $\text{Bi}_{10}\text{Sb}_3\text{Te}_6$ , etc.} nanoparticles after hot pressing for Sample 3 above according to exemplary embodiments of the present technology. The ZT of the nanostructured bismuth antimony telluride will increase with increases in temperature and form a peak at around 100 degrees Celsius.

[0073] As disclosed herein, the inventors' various exemplary methods may be used for making P-type bismuth antimony telluride nanostructured thermoelectric materials {e.g.,  $\text{Bi}_{10}\text{Sb}_3\text{Te}_6$ , etc.} with high ZT {e.g., 0.78, 1.16, 1.39, 1.7, 2, etc.} at room temperature. Additionally, or alternatively, the methods disclosed herein may also or instead be used for making N-type bismuth antimony telluride nanostructured thermoelectric materials {e.g.,  $\text{Bi}_3\text{Sb}_7\text{Te}_6$ ,  $\text{Bi}_2\text{Sb}_3\text{Te}_6$ , etc.} with high ZT {e.g., 0.75, etc.} at room temperature. By way of example, Table 4 below provides electrical conductivity (in Siemens per centimeter (S/cm)), thermal conductivity (in Watts per meter Kelvin (W/mK)), Seebeck coefficient (in microvolts per Kelvin ( $\mu\text{V}/\text{K}$ )) (which is negative for N-type materials), and ZT for a sample of nanostructured bismuth antimony telluride ( $\text{Bi}_{27}\text{Sb}_3\text{Te}_6$ ) N-type thermoelectric material produced using an exemplary method of the present technology. For this sample, ethylene glycol was used for the synthesis of bismuth antimony telluride nanopowders, which were hot pressed without first undergoing argon gas purging surface treatment.

**[0074] Table 4**

Sample ID	Electrical Conductivity (S/cm) ( $\sigma$ )	Thermal Conductivity (W/mK) ( $\kappa$ )	Seebeck Coefficient ( $\mu\text{V/K}$ ) (S)	ZT (at room temperature)
1	439	0.98	-227	0.75

[0075] Accordingly, the inventors hereof have disclosed exemplary embodiments of nanostructured bismuth antimony telluride thermoelectric materials and methods of making the same that may provide one or more (but not necessarily any or all) of the following advantages. For example, exemplary embodiments disclosed herein provide a chemical route synthesis of powder and retention of nanostructure after sintering. The exemplary nanostructured bismuth antimony telluride thermoelectric materials disclosed herein have a high Seebeck coefficient, low thermal conductivity, and a high ZT. Also, exemplary embodiments of the methods of making nanostructured bismuth antimony telluride thermoelectric materials are scalable and amenable for large scale synthesis, such that the inventors' nanostructured bulk bismuth antimony telluride is economically viable to produce in industrial scale. Exemplary embodiments also provide good compositional homogeneity in powders by synthesizing nanoparticles by a bottom up approach in which respective salts and powders were in solutions. Precipitation of bismuth antimony telluride from solution results in very homogeneous composition. This may be shown, for example, by EDS (Energy Dispersive X-Ray Spectroscopy) analysis from different spots of a same sample, and the same may also be reflected in the Seebeck measurement. The Seebeck measurement from a different area in the same sample shows very minimal variation, which results imply compositional homogeneity prevailed throughout that sample.

[0078] Example embodiments are provided so that this disclosure will be thorough, and will fully convey the scope to those who are skilled in the art. Numerous specific details are set forth such as examples of specific components, devices, and methods, to provide a thorough understanding of embodiments of the present



disclosure. It will be apparent to those skilled in the art that specific details need not be employed, that example embodiments may be embodied in many different forms, and that neither should be construed to limit the scope of the disclosure. In some example embodiments, well-known processes, well-known device structures, and well-known technologies are not described in detail. In addition, advantages and improvements that may be achieved with one or more exemplary embodiments of the present disclosure are provided for purpose of illustration only and do not limit the scope of the present disclosure, as exemplary embodiments disclosed herein may provide all or none of the above mentioned advantages and improvements and still fall within the scope of the present disclosure.

[0077] Specific dimensions, specific materials, and/or specific shapes disclosed herein are example in nature and do not limit the scope of the present disclosure. The disclosure herein of particular values and particular ranges of values for given parameters are not exclusive of other values and ranges of values that may be useful in one or more of the examples disclosed herein. Moreover, it is envisioned that any two particular values for a specific parameter stated herein may define the endpoints of a range of values that may be suitable for the given parameter (*i.e.*, the disclosure of a first value and a second value for a given parameter can be interpreted as disclosing that any value between the first and second values could also be employed for the given parameter). Similarly, it is envisioned that disclosure of two or more ranges of values for a parameter (whether such ranges are nested, overlapping or distinct) subsume all possible combination of ranges for the value that might be claimed using endpoints of the disclosed ranges.

[0078] The terminology used herein is for the purpose of describing particular example embodiments only and is not intended to be limiting. As used herein, the singular forms "a", "an" and "the" may be intended to include the plural forms as well, unless the context clearly indicates otherwise. The terms "comprises," "comprising," "including," and "having," are inclusive and therefore specify the presence of stated features, integers, steps, operations, elements, and/or components, but do not preclude the presence or addition of one or more other features, integers, steps, operations, elements, components, and/or groups thereof. The method steps, processes, and

operations described herein are not to be construed as necessarily requiring their performance in the particular order discussed or illustrated, unless specifically identified as an order of performance. It is also to be understood that additional or alternative steps may be employed.

[0079] When an element or layer is referred to as being "on", "engaged to", "connected to" or "coupled to" another element or layer, it may be directly on, engaged, connected or coupled to the other element or layer, or intervening elements or layers may be present. In contrast, when an element is referred to as being "directly on," "directly engaged to", "directly connected to" or "directly coupled to" another element or layer, there may be no intervening elements or layers present. Other words used to describe the relationship between elements should be interpreted in a like fashion (*e.g.*, "between" versus "directly between," "adjacent" versus "directly adjacent," *etc.*). As used herein, the term "and/or" includes any and all combinations of one or more of the associated listed items. The term "about" when applied to values indicates that the calculation or the measurement allows some slight imprecision in the value (with some approach to exactness in the value; approximately or reasonably close to the value; nearly). If, for some reason, the imprecision provided by "about" is not otherwise understood in the art with this ordinary meaning, then "about" as used herein indicates at least variations that may arise from ordinary methods of measuring or using such parameters. For example, the terms "generally", "about", and "substantially" may be used herein to mean within manufacturing tolerances.

[0080] Although the terms first, second, third, *etc.* may be used herein to describe various elements, components, regions, layers and/or sections, these elements, components, regions, layers and/or sections should not be limited by these terms. These terms may be only used to distinguish one element, component, region, layer or section from another region, layer or section. Terms such as "first," "second," and other numerical terms when used herein do not imply a sequence or order unless clearly indicated by the context. Thus, a first element, component, region, layer or section discussed below could be termed a second element, component, region, layer or section without departing from the teachings of the example embodiments.

[0081] Spatially relative terms, such as "inner," "outer," "beneath", "below", "lower", "above", "upper" and the like, may be used herein for ease of description to describe one element or feature's relationship to another element(s) or feature(s) as illustrated in the figures. Spatially relative terms may be intended to encompass different orientations of the device in use or operation in addition to the orientation depicted in the figures. For example, if the device in the figures is turned over, elements described as "below" or "beneath" other elements or features would then be oriented "above" the other elements or features. Thus, the example term "below" can encompass both an orientation of above and below. The device may be otherwise oriented (rotated 90 degrees or at other orientations) and the spatially relative descriptors used herein interpreted accordingly.

[0082] The foregoing description of the embodiments has been provided for purposes of illustration and description. It is not intended to be exhaustive or to limit the disclosure. Individual elements, intended or stated uses, or features of a particular embodiment are generally not limited to that particular embodiment, but, where applicable, are interchangeable and can be used in a selected embodiment, even if not specifically shown or described. The same may also be varied in many ways. Such variations are not to be regarded as a departure from the disclosure, and all such modifications are intended to be included within the scope of the disclosure.

## CLAIMS

What is claimed is:

1. A thermoelectric nano-bulk composite material comprising:  
a matrix including nanostructured bismuth antimony telluride; and  
bulk bismuth antimony telluride in the matrix;  
wherein a weight percentage ratio of the nanostructured bismuth antimony telluride to the bulk bismuth antimony telluride is at least one to one or higher.

2. The thermoelectric nano-bulk composite material of any one of the preceding claims, wherein:

the thermoelectric nano-bulk composite material includes at least 50 percent by weight of the nanostructured bismuth antimony telluride, and no more than 50 percent by weight of the bulk bismuth antimony telluride; and/or

the thermoelectric nano-bulk composite material includes more than 50 percent by weight of the nanostructured bismuth antimony telluride nanostructures; and/or

the weight percentage ratio of the nanostructured bismuth antimony telluride to the bulk bismuth antimony telluride is greater than one to one; and/or

the thermoelectric nano-bulk composite material includes between 50 and 90 percent by weight of the nanostructured bismuth antimony telluride.

3. The thermoelectric nano-bulk composite material of any one of the preceding claims, wherein the matrix comprises nanostructured sheets of bismuth antimony telluride that are in contact with the bulk bismuth antimony telluride, whereby the presence of the bulk bismuth antimony telluride in the matrix provides better connectivity between the nanostructured sheets of bismuth antimony telluride and forms randomized short range sheet nanostructure in the thermoelectric nano-bulk composite material.

4. The thermoelectric nano-bulk composite material of any one of the preceding claims, wherein:

the thermoelectric nano-bulk composite material has a dimensionless figure of merit (ZT) of at least 1.26 at a room temperature of 300 Kelvin; and/or

the thermoelectric nano-bulk composite material has better compressive strength than the bulk bismuth antimony telluride; and/or

the thermoelectric nano-bulk composite material has a lower thermal conductivity than the bulk bismuth antimony telluride; and/or

the thermoelectric nano-bulk composite material has a thermal conductivity less than or equal to a thermal conductivity of the parent as prepared nanoparticle powder.

5. The thermoelectric nano-bulk composite material of any one of the preceding claims, wherein:

the matrix consists only of the nanostructured bismuth antimony telluride; and/or

the bulk bismuth antimony telluride comprises bismuth antimony telluride microparticles that are an inclusion in the matrix.

6. The thermoelectric nano-bulk composite material of any one of the preceding claims, wherein the thermoelectric nano-bulk composite material is a reverse nano-bulk composite in which the nanostructured bismuth antimony telluride is used as the matrix and the bulk bismuth antimony telluride is an inclusion in the matrix.

7. The thermoelectric nano-bulk composite material of any one of the preceding claims, wherein:

the matrix comprises a nanostructured sheet of bismuth antimony telluride and/or bismuth antimony telluride nanoparticles; and/or

the matrix comprises nanostructured bismuth antimony telluride ( $\text{Bi}_{40-x}\text{SbxTe}_{100}$ ) where X has a value of at least 25 but not more than 32; and/or

the thermoelectric material is a P-type thermoelectric material; and/or  
the matrix comprises nanostructured bismuth antimony telluride  
( $\text{Bi}_{0.4}\text{Sb}_{1.6}\text{Te}_3$ ).

8. The thermoelectric nano-bulk composite material of any one of the preceding claims, wherein the thermoelectric nano-bulk composite material has:

a Seebeck coefficient within a range from 236 to 273 microvolts per Kelvin ( $\mu\text{V}/\text{K}$ ); and/or

a ZT within a range from 1.26 and 1.51 at a room temperature of 300 Kelvin; and/or

a thermal conductivity within a range from 0.80 Watts per meter Kelvin ( $\text{W}/\text{mK}$ ) to .99  $\text{W}/\text{mK}$ ; and/or

an electrical conductivity within a range from 511 Siemens per centimeter ( $\text{S}/\text{cm}$ ) to 823  $\text{S}/\text{cm}$ .

9. A thermoelectric module comprising the thermoelectric nano-bulk composite material of any one of the preceding claims.

10. The thermoelectric module of claim 9, wherein:

the thermoelectric nano-bulk composite material is a P-type thermoelectric material; and

the thermoelectric module further includes an N-type thermoelectric material.

11. A method of making a thermoelectric nano-bulk composite material, the method comprising incorporating bulk bismuth antimony telluride into a matrix including nanostructured bismuth antimony telluride, such that a weight percentage ratio of the nanostructured bismuth antimony telluride to the bulk bismuth antimony telluride is at least one to one or higher.

12. The method of claim 11, wherein the method includes hot pressing the nanostructured bismuth antimony telluride in the presence of the bulk bismuth antimony telluride.

13. The method of claim 11 or 12, wherein the method includes incorporating an amount of bulk bismuth antimony telluride into the matrix such that:

the thermoelectric nano-bulk composite material includes at least 50 percent by weight of the nanostructured bismuth antimony telluride, and no more than 50 percent by weight of the bulk bismuth antimony telluride; and/or

the thermoelectric nano-bulk composite material includes more than 50 percent by weight of the nanostructured bismuth antimony telluride nanostructures; and/or

the weight percentage ratio of the nanostructured bismuth antimony telluride to the bulk bismuth antimony telluride is greater than one to one; and/or

the thermoelectric nano-bulk composite material includes between 50 and 90 percent by weight of the nanostructured bismuth antimony telluride.

14. The method of any one of claims 11 to 13, wherein:  
the matrix comprises nanostructured sheets of bismuth antimony telluride;  
and

the method includes hot pressing the nanostructured sheets of bismuth antimony telluride in the presence of the bulk bismuth antimony telluride such that the order of the sheet nanostructure is perturbed thereby forming highly randomized short range sheet structures.

15. The method of any one of claims 11 to 14, wherein the matrix comprises:

a nanostructured sheet of bismuth antimony telluride and/or bismuth antimony telluride nanoparticles; and/or

nanostructured bismuth antimony telluride ( $\text{Bi}_{4_0-x}\text{Sb}_x\text{Te}_6$ ) where X has a value of at least 25 but not more than 32; and/or

nanostructured bismuth antimony telluride ( $\text{Bi}_{0.4}\text{Sb}_{1.6}\text{Te}_3$ ).

16. The method of any one of claims 11 to 15, wherein the method includes:

synthesizing the nanostructured bismuth antimony telluride via a wet chemical route; and

synthesizing the bulk bismuth antimony telluride via a solid state synthesis.

17. The method of any one of claims 11 to 16, wherein:

the nanostructured bismuth antimony telluride comprises a nanostructured sheet of bismuth antimony telluride nanoparticles; and

the method includes:

synthesizing bismuth antimony telluride nanoparticles using bismuth powder and salts of tellurium and antimony; and

densifying the synthesized bismuth antimony telluride nanoparticles into the nanostructured sheet of bismuth antimony telluride nanoparticles.

18. A thermoelectric material comprising a nanostructured sheet of bismuth antimony telluride nanoparticles, the thermoelectric material having:

a dimensionless figure of merit (ZT) of at least 2 at a room temperature of 300 Kelvin; and/or

a Seebeck coefficient of at least 276 microvolts per Kelvin ( $\mu\text{V}/\text{K}$ ).



19. The thermoelectric material of claim 18, wherein:  
the nanostructured sheet of bismuth antimony telluride nanoparticles includes a 2D sheet nanostructure; and/or  
the nanostructured sheet of bismuth antimony telluride nanoparticles comprises a 2D nanostructured sheet having a thickness dimension within a range from 30 nanometers (nm) to 50 nm; and/or  
the nanoparticles comprise bismuth antimony telluride ( $\text{Bi}_{4-x}\text{SbxTe}_6$ ) where X has a value of at least 25 but not more than 32; and/or  
the nanoparticles comprise bismuth antimony telluride ( $\text{Bi}_{10}\text{Sb}_{30}\text{Te}_6$ )-

20. The thermoelectric material of claim 18 or 19, wherein the thermoelectric material is a P-type thermoelectric material having a Seebeck coefficient of at least 276 microvolts per Kelvin ( $\mu\text{V}/\text{K}$ ) and a dimensionless figure of merit (ZT) of at least 2 at a room temperature of 300 Kelvin.

21. The thermoelectric material of any one of the preceding claims, wherein the thermoelectric material has:

a Seebeck coefficient within a range from 276 to 311 microvolts per Kelvin ( $\mu\text{V}/\text{K}$ ); and/or

a ZT within a range from 0.78 and 2 at a room temperature of 300 Kelvin; and/or

a thermal conductivity within a range from 0.76 Watts per meter Kelvin ( $\text{W}/\text{mK}$ ) to 1.0  $\text{W}/\text{mK}$ ; and/or

an electrical conductivity within a range from 264 Siemens per centimeter ( $\text{S}/\text{cm}$ ) to 882  $\text{S}/\text{cm}$ .

22. A method for making a nanostructured sheet of bismuth antimony telluride nanoparticles having a dimensionless figure of merit (ZT) of at least 2 at a room temperature of 300 Kelvin and/or a Seebeck coefficient of at least 276 microvolts per Kelvin ( $\mu\text{V}/\text{K}$ ), the method comprising:

synthesizing bismuth antimony telluride nanoparticles using bismuth powder and salts of tellurium and antimony; and

densifying the synthesized bismuth antimony telluride nanoparticles into a nanostructured sheet of bismuth antimony telluride nanoparticles.

23. A method for making a thermoelectric material comprising a nanostructured sheet of bismuth antimony telluride nanoparticles, the method comprising:

synthesizing bismuth antimony telluride nanoparticles using bismuth powder and salts of tellurium and antimony; and

densifying the synthesized bismuth antimony telluride nanoparticles into a nanostructured sheet.

24. The method of claim 22 or 23, wherein synthesizing bismuth antimony telluride nanoparticles is performed via a wet chemical route including a single step synthesis of bismuth antimony telluride via a simultaneous reduction and an alloy formation.

25. The method of any one of claims 22 to 24, wherein synthesizing bismuth antimony telluride nanoparticles includes reacting the bismuth powder and salts of tellurium and antimony in a diol.

26. The method of any one of claims 22 to 25, wherein synthesizing bismuth antimony telluride nanoparticles includes:

dissolving telluric acid and antimony acetate in a diol;

dissolving bismuth metal powder in concentrated nitric acid;

combining the dissolved telluric acid and antimony acetate in 1,5-pentanediol or ethylene glycol with the dissolved bismuth metal powder in concentrated nitric acid to form a combined mixture; and

adding a reducing agent to the combined mixture.

27. The method of any one of claims 22 to 26, wherein:  
the method includes surface treating the synthesized bismuth antimony telluride nanoparticles by exposure to argon gas containing oxygen and moisture, prior to densifying; and  
densifying synthesized bismuth antimony telluride nanoparticles comprises hot pressing the synthesized bismuth antimony telluride nanoparticles into a nanostructured sheet.

28. The method of claim 27, wherein:  
the hot pressing is performed at a temperature from 300 °C to 500 °C;  
and/or  
the hot pressing is performed at a pressure from 150 kilograms per square centimeter ( $\text{kg}/\text{cm}^2$ ) to 400  $\text{kg}/\text{cm}^2$ ; and/or  
the hot pressing is performed for a duration between 2 hours to 4 hours;  
and/or  
the hot pressing includes increasing the pressure at a rate of 15  $\text{kg}/\text{cm}^2$  to 20  $\text{kg}/\text{cm}^2$  per minute until a final pressure is reached.

29. The method of any one of claims 22 to 28, wherein:  
synthesizing bismuth antimony telluride nanoparticles is performed via a wet chemical route including a single step synthesis of bismuth antimony telluride via a simultaneous reduction and an alloy formation; and/or  
the nanostructured sheet of bismuth antimony telluride nanoparticles comprises a P-type thermoelectric material having a Seebeck coefficient of at least 276 microvolts per Kelvin ( $\mu\text{V}/\text{K}$ ) and a dimensionless figure of merit (ZT) of at least 2 at a room temperature of 300 Kelvin; and/or  
the nanostructured sheet of bismuth antimony telluride nanoparticles includes a 2D sheet nanostructure; and/or  
the nanostructured sheet of bismuth antimony telluride nanoparticles comprises a 2D nanostructured sheet having a thickness dimension within a range from 30 nanometers (nm) to 50 nm; and/or

the nanoparticles comprises bismuth antimony telluride ( $\text{Bi}_{40-x}\text{Sb}_x\text{Te}_{60}$ ) where X has a value of at least 25 but not more than 32.

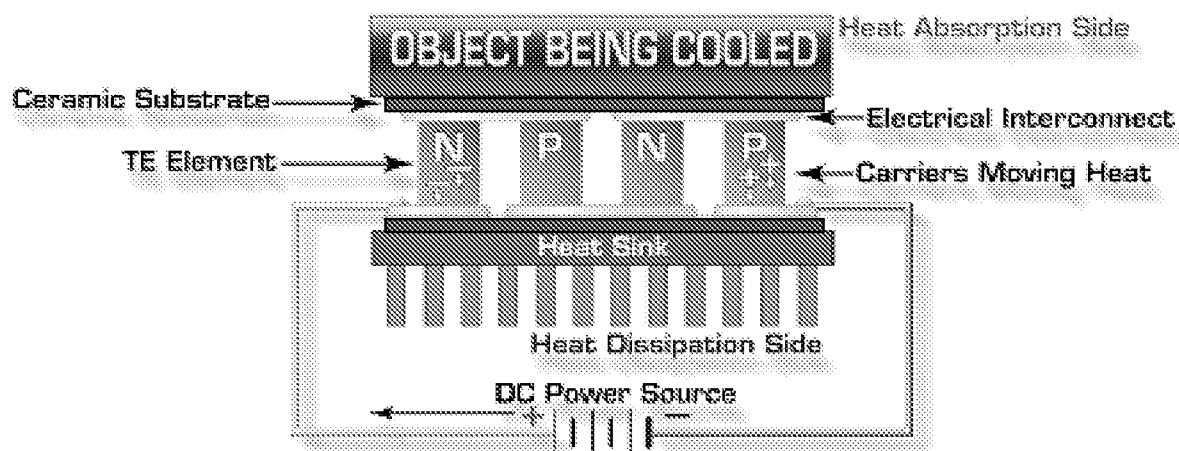


FIG. 1

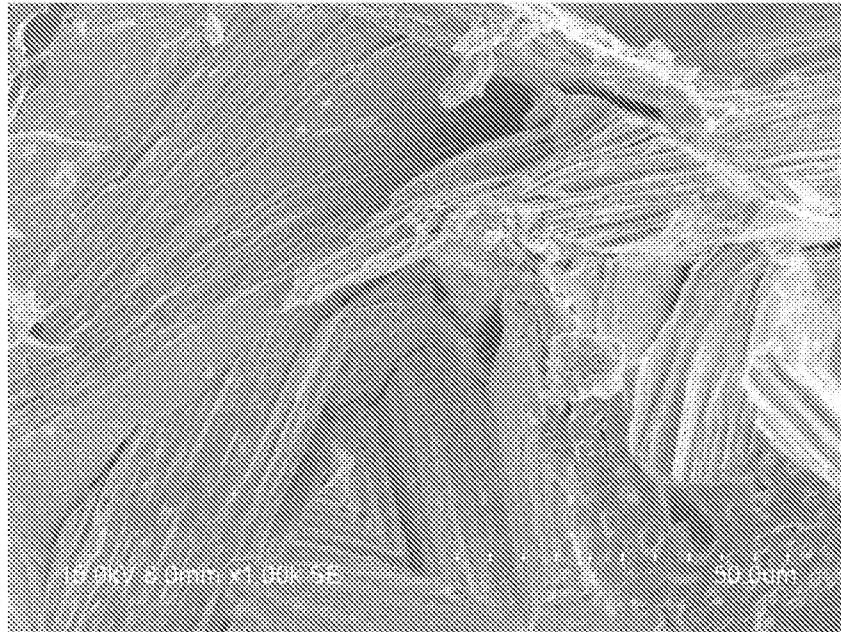


FIG. 2

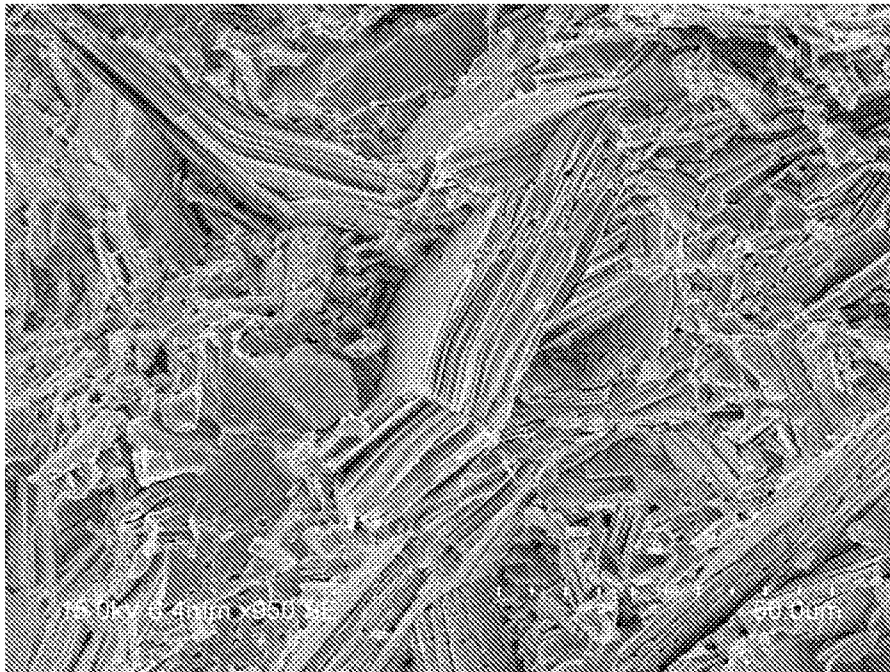


FIG. 3A

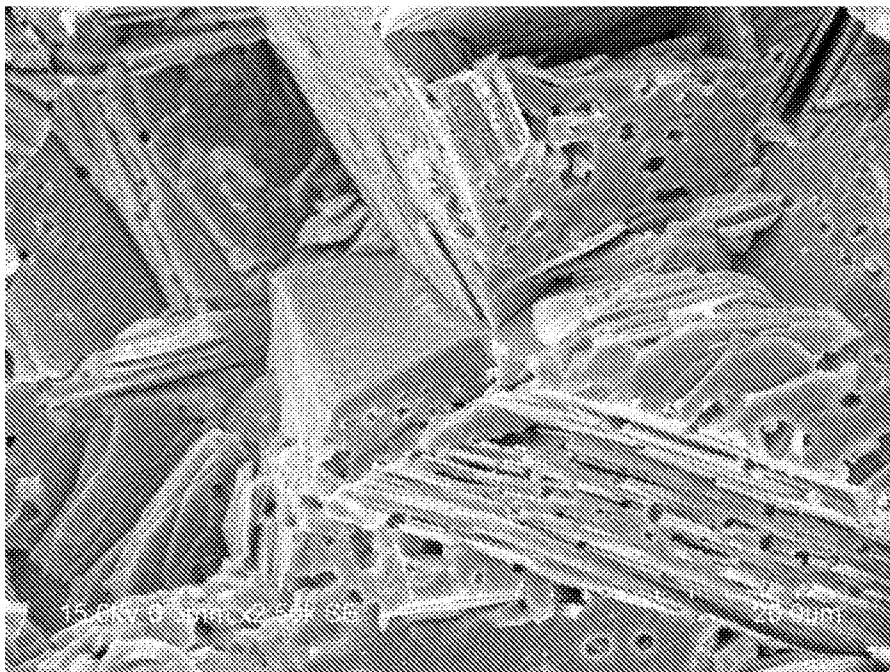


FIG. 3B

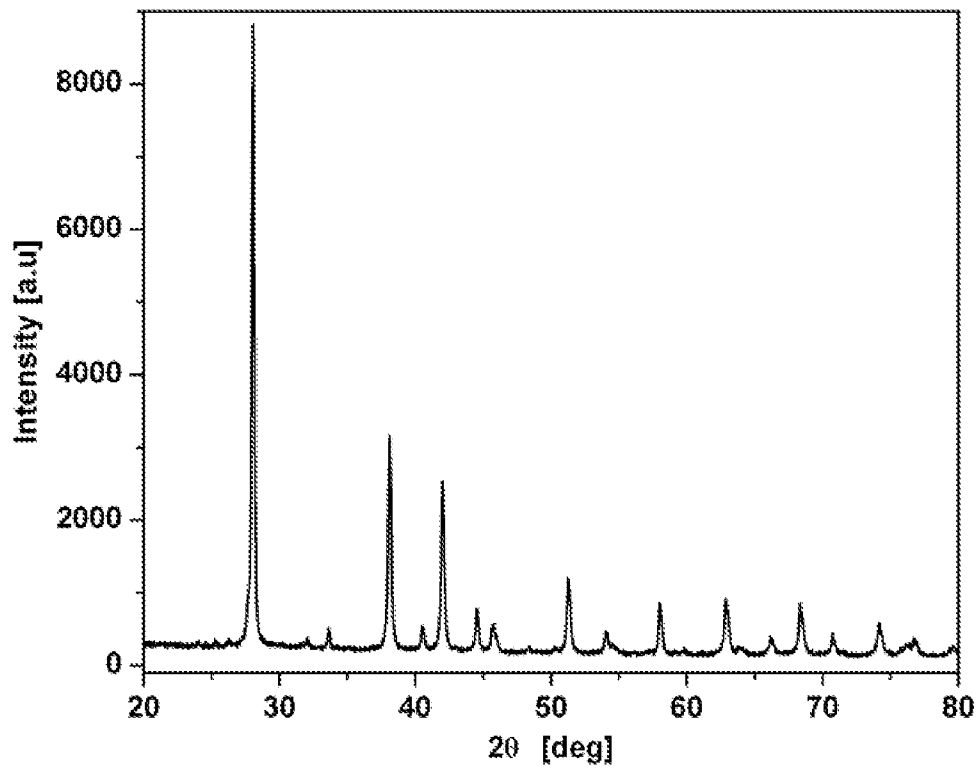


FIG. 4



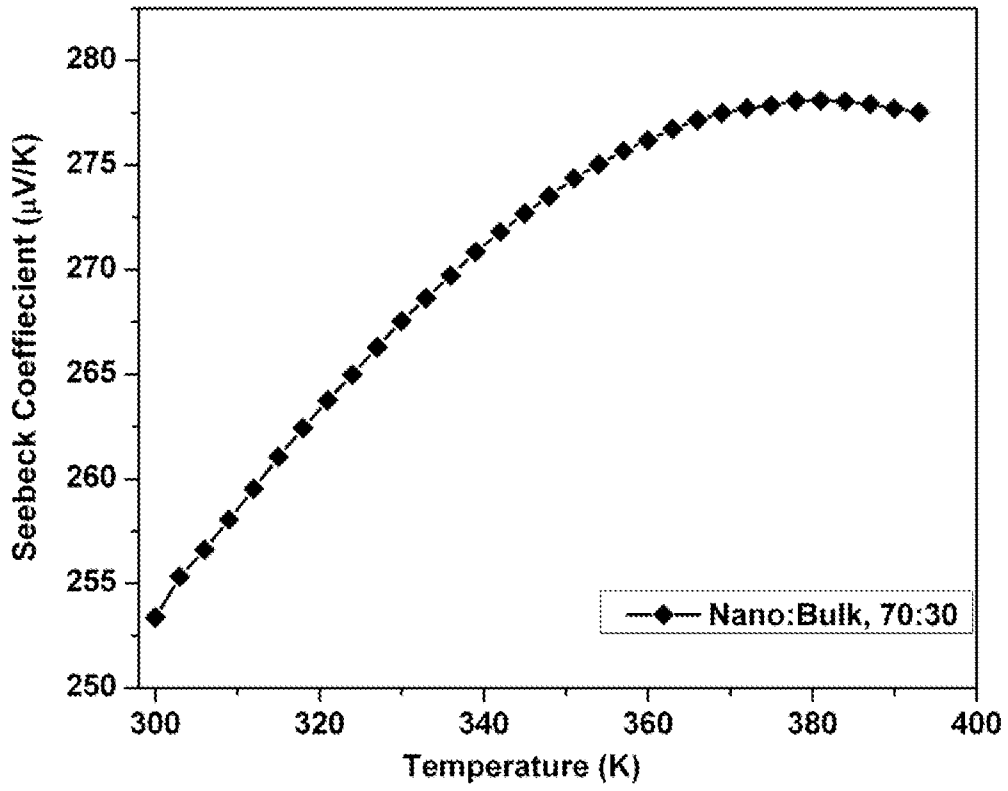


FIG. 5

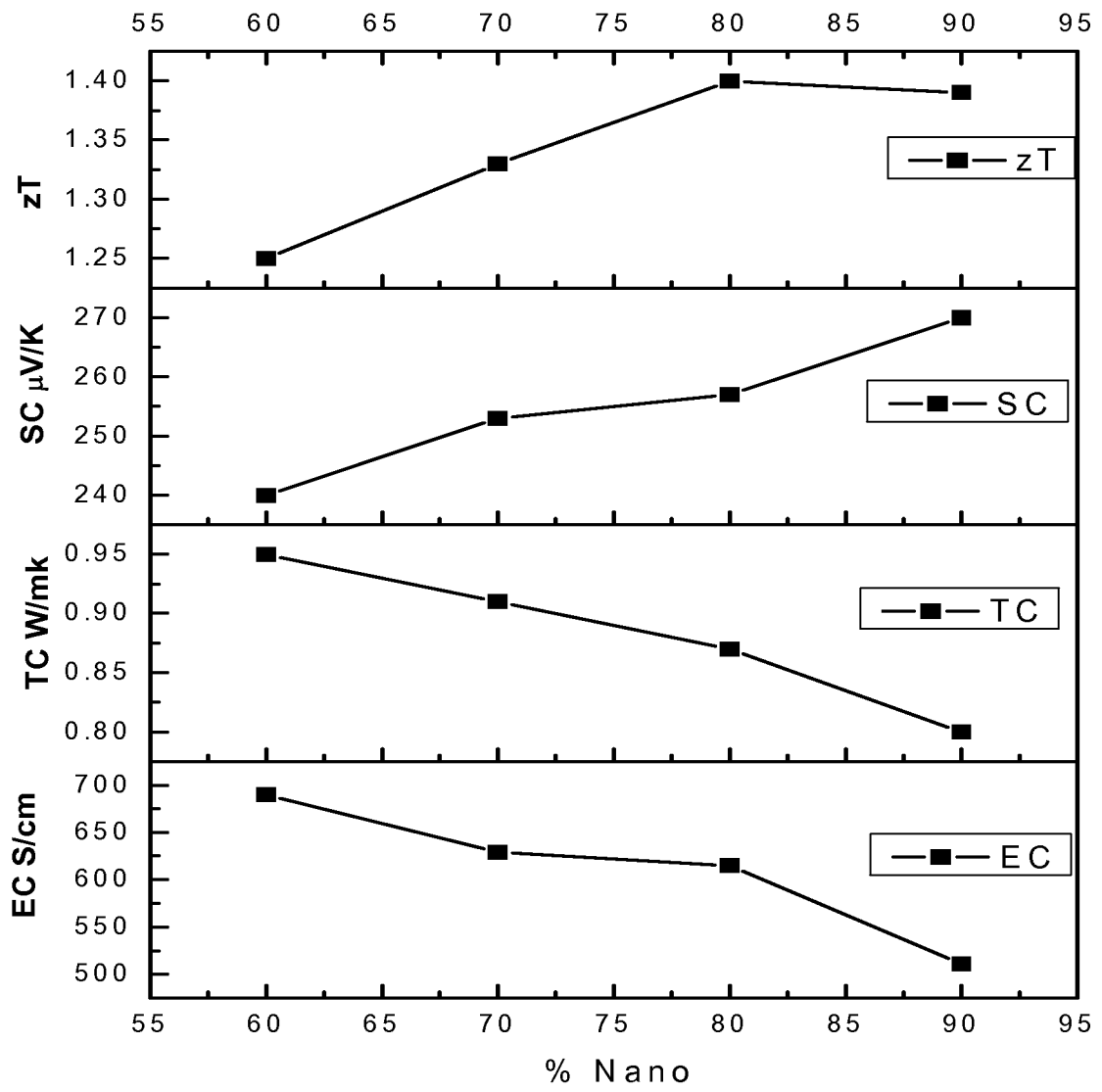


FIG. 6

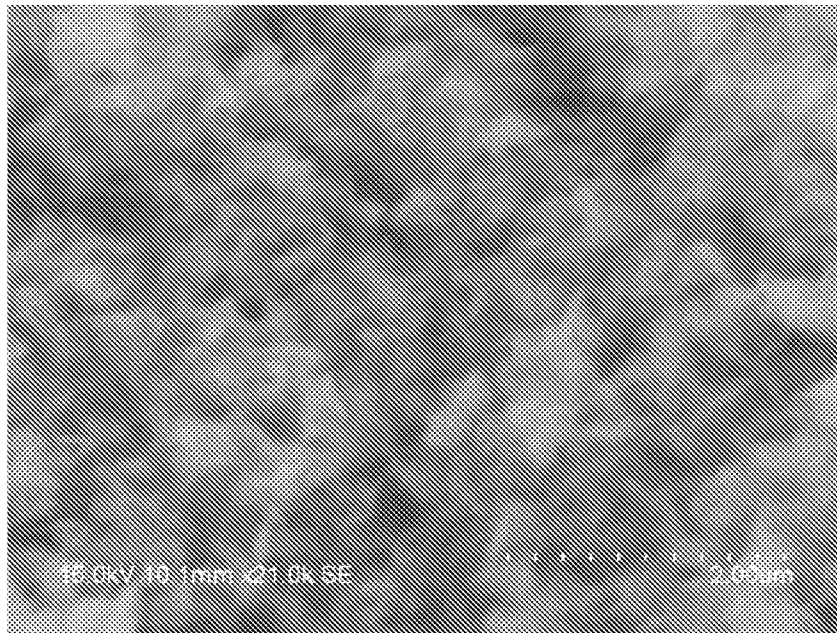


FIG. 7A

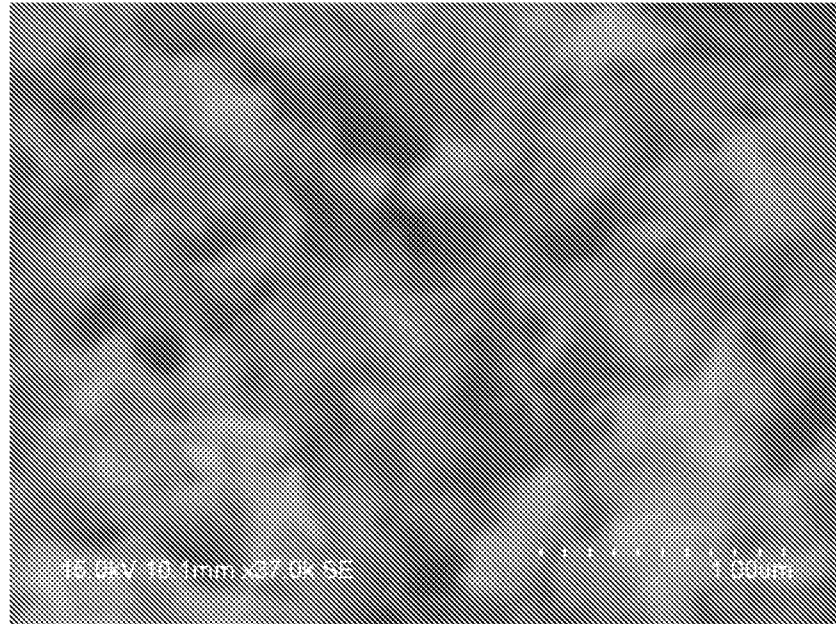


FIG. 7B

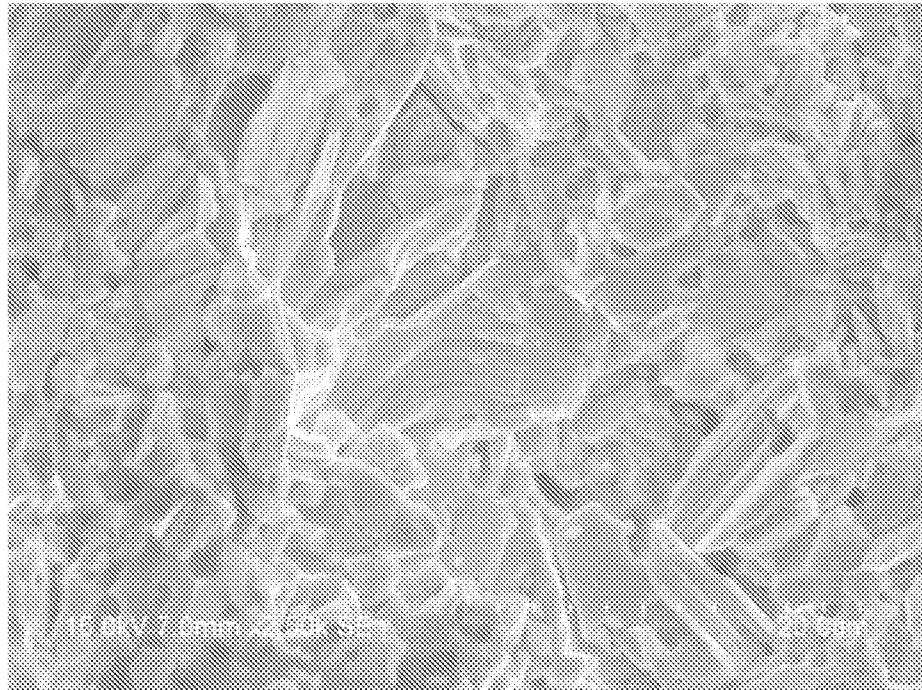


FIG. 8A

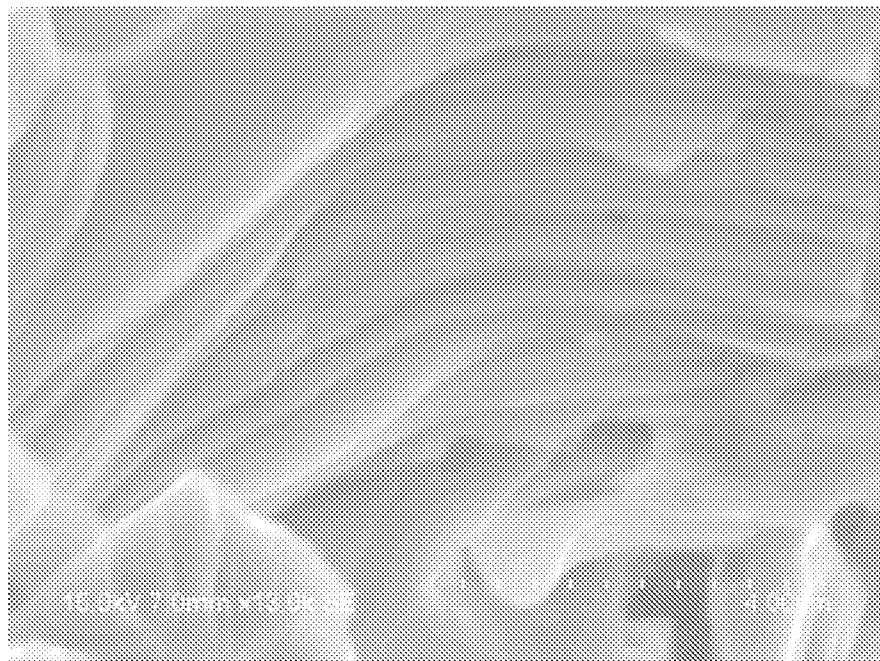


FIG. 8B

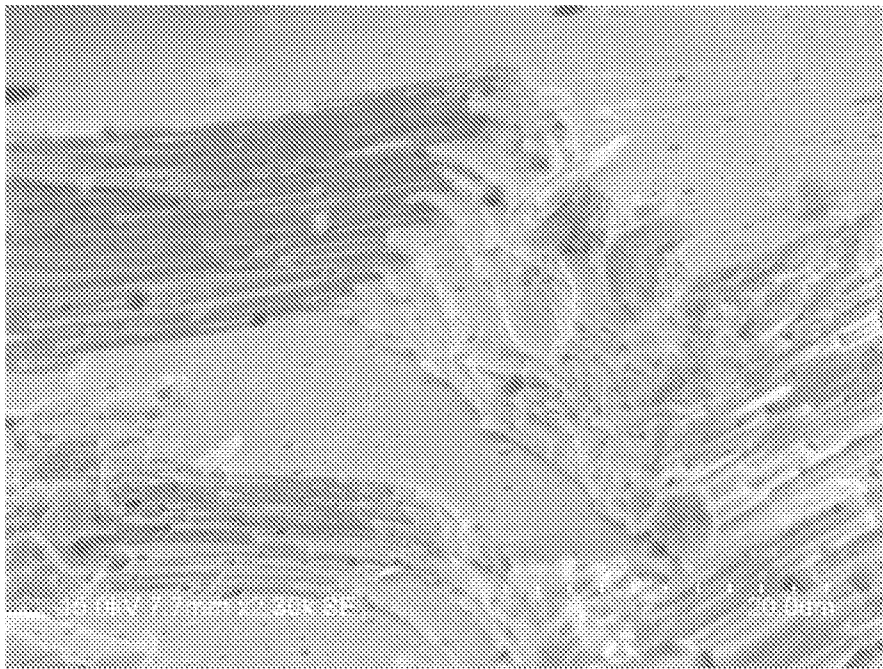


FIG. 9A

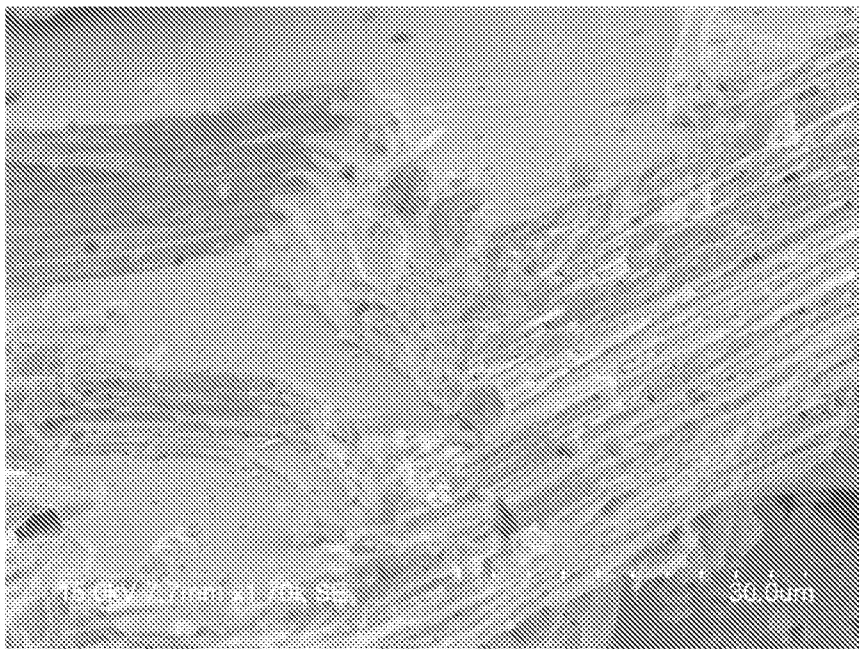


FIG. 9B

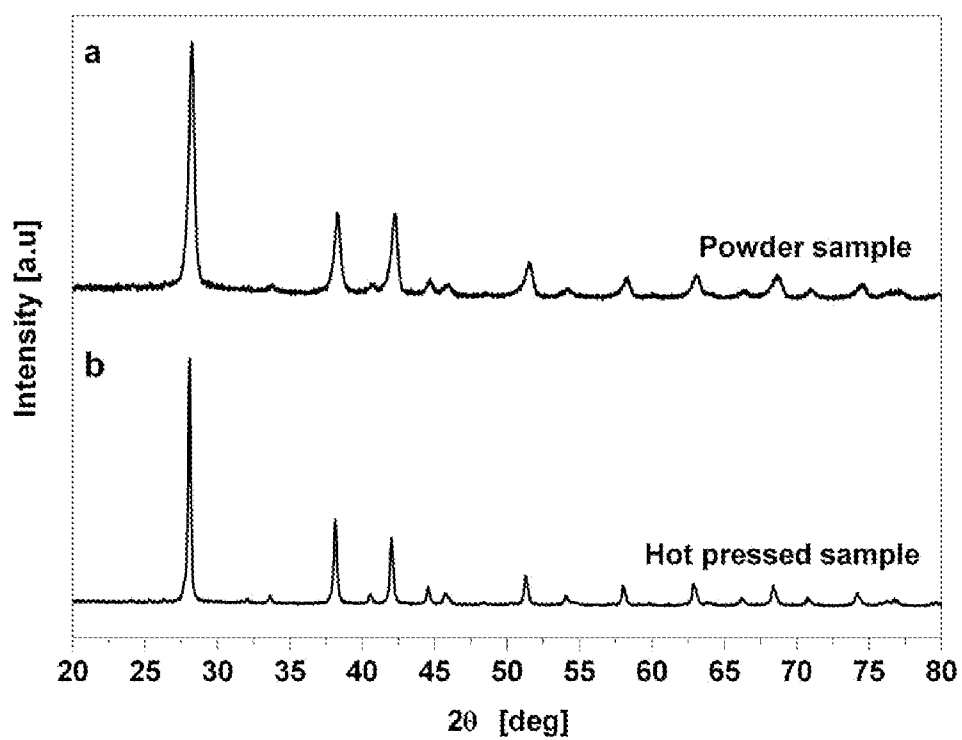


FIG. 10

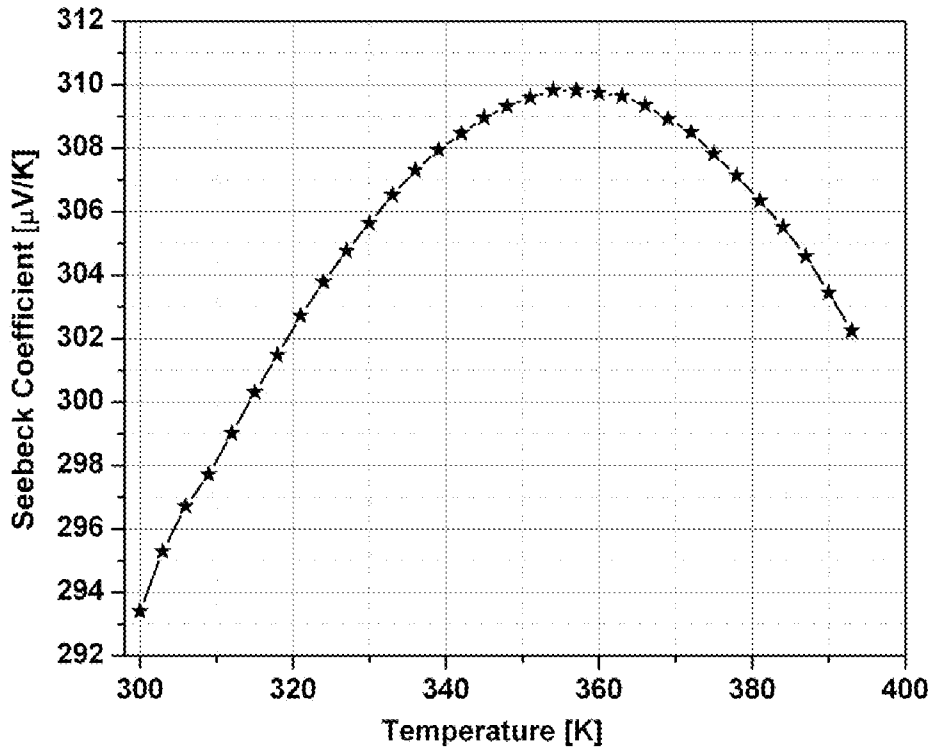


FIG. 11

## INTERNATIONAL SEARCH REPORT

International application No.  
**PCT/US2013/042537****A. CLASSIFICATION OF SUBJECT MATTER****H01L 35/18(2006.01)i**

According to International Patent Classification (IPC) or to both national classification and IPC

**B. FIELDS SEARCHED**Minimum documentation searched (classification system followed by classification symbols)  
H01L 35/18; H01L 35/16; H01L 35/32; H01L 35/34; C01B 19/04Documentation searched other than minimum documentation to the extent that such documents are included in the fields searched  
Korean utility models and applications for utility models  
Japanese utility models and applications for utility modelsElectronic data base consulted during the international search (name of data base and, where practicable, search terms used)  
eKOMPASS(KIPO internal) & keywords: bismuth antimony telluride, nano-bulk, nanostructure, bulk, weight percentage, ratio, sheet**C. DOCUMENTS CONSIDERED TO BE RELEVANT**

Category*	Citation of document, with indication, where appropriate, of the relevant passages	Relevant to claim No.
X A	wo 2008-140596 A2 (MASSACHUSETTS INSTITUTE OF TECHNOLOGY) 20 November 2008 See abstract ; claims 1, 22, 39; and figures 1A, 1B.	18-20 ,22-24 1-3 ,11-13
A	US 2012-0145212 A1 (ARUP PURKAYASTHA et al.) 14 June 2012 See abstract ; claims 1, 2; and paragraph [0026] ,	1-3, 11-13 ,18-20 ,22-24
A	BED POUDEL et al. "High-Thermoelectric Performance of Nanostructured Bismuth Antimony Telluride Bulk Alloys " Science. 2 May 2008, Vol. 320, No. 5876, pages 634-638 See abstract ; pages 3-5 ; figures 3A-3F.	1-3, 11-13 ,18-20 ,22-24
A	WENJIE XIE et al. "Unique nanostructures and enhanced thermoelectric performance of melt-spun BiSbTe alloys " Applied Physics Letters . 12 March 2009, Vol. 94, No. 102111, pages 102111-1 ~ 102111-3 See abstract ; pages 1-3; and figures 3A, 3B.	1-3, 11-13 ,18-20 ,22-24
A	WEILI REN et al. "The effect of the precursor nanopowder size on the thermoelectric properties of nanostructured Bi-Sb-Te bulk materials" Physica B. 15 December 2010, Vol. 405, No. 24, Pages 4931-4936 See abstract ; pages 1-3; and figures 5A-5D.	1-3, 11-13 ,18-20 ,22-24



Further documents are listed in the continuation of Box C.



See patent family annex.

\* Special categories of cited documents:

"A" document defining the general state of the art which is not considered to be of particular relevance

"E" earlier application or patent but published on or after the international filing date

"L" document which may throw doubts on priority claim(s) or which is cited to establish the publication date of citation or other special reason (as specified)

"O" document referring to an oral disclosure, use, exhibition or other means

"P" document published prior to the international filing date but later than the priority date claimed

"T" later document published after the international filing date or priority date and not in conflict with the application but cited to understand the principle or theory underlying the invention

"X" document of particular relevance; the claimed invention cannot be considered novel or cannot be considered to involve an inventive step when the document is taken alone

"Y" document of particular relevance; the claimed invention cannot be considered to involve an inventive step when the document is combined with one or more other such documents, such combination being obvious to a person skilled in the art

"&amp;" document member of the same patent family


Date of the actual completion of the international search

30 August 2013 (30.08.2013)

Date of mailing of the international search report

**30 August 2013 (30.08.2013)**

Name and mailing address of the ISA/KR


 Korean Intellectual Property Office  
189 Cheongsang-ro, Seo-gu, Daejeon Metropolitan City,  
302-701, Republic of Korea

Facsimile No. +82-42-472-7140

Authorized officer

LEE Dong Yun

Telephone No. +82-42-481-8734





**Box No. II Observations where certain claims were found unsearchable (Continuation of item 2 of first sheet)**

This international search report has not been established in respect of certain claims under Article 17(2)(a) for the following reasons:

1.  Claims NOB.:  
because they relate to subject matter not required to be searched by this Authority, namely:
  
2.  Claims Nos.: 10, 28  
because they relate to parts of the international application that do not comply with the prescribed requirements to such an extent that no meaningful international search can be carried out, specifically:  
Claims 10, 28 have been drafted as dependent claims on multiple dependent claims. Lack of clarity of the claims as a whole arises, since a plurality of dependent claims make it difficult to determine the matter for which protection is sought.
  
3.  Claims Nos.: 4-9, 14-17, 21, 25-27, 29  
because they are dependent claims and are not drafted in accordance with the second and third sentences of Rule 6.4(a).

**Box No. III Observations where unity of invention is lacking (Continuation of item 3 of first sheet)**

This International Searching Authority found multiple inventions in this international application, as follows:

1.  As all required additional search fees were timely paid by the applicant, this international search report covers all searchable claims.
  
2.  As all searchable claims could be searched without effort justifying an additional fee, this Authority did not invite payment of any additional fee.
  
3.  As only some of the required additional search fees were timely paid by the applicant, this international search report covers only those claims for which fees were paid, specifically claims Nos.:
  
  
  
  
  
  
  
4.  No required additional search fees were timely paid by the applicant. Consequently, this international search report is restricted to the invention first mentioned in the claims; it is covered by claims Nos.:

**Remark on Protest**

The additional search fees were accompanied by the applicant's protest and, where applicable, the payment of a protest fee.

The additional search fees were accompanied by the applicant's protest but the applicable protest fee was not paid within the time limit specified in the invitation.

No protest accompanied the payment of additional search fees.

**INTERNATIONAL SEARCH REPORT**

Information on patent family members

International application No.

**PCT7US2013/042537**

Patent document cited in search report	Publication date	Patent family member(s)	Publication date
WO 2008-140596 A2	20/11/2008	CN 101803050 A	11/08/2010
		JP 2010-512011 A	15/04/2010
		KR 10-2009-0110831 A	22/10/2009
		wo 2008-140596 A3	30/12/2009
US 2012-0145212 A1	14/06/2012	CN 102598893 A	18/07/2012
		KR 10-2012-0064680 A	19/06/2012
		KR 10-2012-0089460 A	10/08/2012
		US 2012-0153239 A1	21/06/2012
		wo 2011-022188 A2	24/02/2011
		wo 2011-022188 A3	16/06/2011
		wo 2011-022189 A2	24/02/2011
		wo 2011-022189 A3	16/06/2011